

Effect of Cu/Zn ratios and Zr, Mn promoters on CuO/ZnO-based catalysts for methanol synthesis via hydrogenation of CO and CO₂



A Thesis Submitted in Partial Fulfillment of the Requirements
for the Degree of Master of Engineering in Chemical Engineering

Department of Chemical Engineering

FACULTY OF ENGINEERING

Chulalongkorn University

Academic Year 2020

Copyright of Chulalongkorn University

ผลของอัตราส่วนคอปเปอร์ต่อซิงค์ และตัวส่งเสริมเซอร์โคเนียม แมงกานีสต่อตัวเร่งปฏิกิริยาที่มี
องค์ประกอบของ CuO/ZnO สำหรับการสังเคราะห์เมทานอลโดยไฮโดรจิเนชันของ
คาร์บอนมอนอกไซด์และคาร์บอนไดออกไซด์



วิทยานิพนธ์นี้เป็นส่วนหนึ่งของการศึกษาตามหลักสูตรปริญญาวิศวกรรมศาสตรมหาบัณฑิต
สาขาวิชาวิศวกรรมเคมี ภาควิชาวิศวกรรมเคมี
คณะวิศวกรรมศาสตร์ จุฬาลงกรณ์มหาวิทยาลัย
ปีการศึกษา 2563
ลิขสิทธิ์ของจุฬาลงกรณ์มหาวิทยาลัย

Thesis Title	Effect of Cu/Zn ratios and Zr, Mn promoters on CuO/ZnO-based catalysts for methanol synthesis via hydrogenation of CO and CO ₂
By	Miss Phapatchaya Phonrat
Field of Study	Chemical Engineering
Thesis Advisor	Professor BUNJERD JONGSOMJIT, Ph.D.

Accepted by the FACULTY OF ENGINEERING, Chulalongkorn University in Partial Fulfillment of the Requirement for the Master of Engineering

..... Dean of the FACULTY OF
ENGINEERING
(Professor SUPOT TEACHAVORASINSKUN, D.Eng.)

THESIS COMMITTEE

..... Chairman
(Associate Professor PATTARAPORN KIM, Ph.D.)

..... Thesis Advisor
(Professor BUNJERD JONGSOMJIT, Ph.D.)

..... Examiner
(Professor JOONGJAI PANPRANOT, Ph.D.)

..... External Examiner
(Assistant Professor Sasiradee Jantasee, Ph.D.)

ปัทมา พหลรัฐ : ผลของอัตราส่วนคอปเปอร์ต่อซิงค์ และตัวส่งเสริมเซอร์โคเนียม แมงกานีส ต่อตัวเร่งปฏิกิริยาที่มีองค์ประกอบของ CuO/ZnO สำหรับการสังเคราะห์เมทานอลโดยไฮโดรจิเนชันของคาร์บอนมอนอกไซด์และคาร์บอนไดออกไซด์. (Effect of Cu/Zn ratios and Zr, Mn promoters on CuO/ZnO-based catalysts for methanol synthesis via hydrogenation of CO and CO₂) อ.ที่ปรึกษาหลัก : ศ. ดร.บรรเจิด จงสมจิตร

งานวิจัยนี้มีวัตถุประสงค์เพื่อศึกษาตัวเร่งปฏิกิริยาคอปเปอร์ออกไซด์ ซิงค์ออกไซด์ และอะลูมิเนียมออกไซด์ (CZA catalyst) ที่มีอัตราส่วนน้ำหนักของคอปเปอร์ต่อซิงค์แตกต่างกันคือ CZA-0.5, CZA-1, CZA-2 and CZA-3.5 ซึ่งมีอัตราส่วนโดยน้ำหนักของคอปเปอร์ต่อซิงค์เท่ากับ 0.5, 1, 2 และ 3.5 ตามลำดับ ตัวเร่งปฏิกิริยาถูกเตรียมด้วยวิธีการตกตะกอนร่วม นำตัวเร่งปฏิกิริยาไปวิเคราะห์คุณลักษณะทางกายภาพและทางเคมีด้วยเทคนิค N₂ adsorption, CO-Chemisorption, SEM-EDX, ICP-MS, XRD, XPS, H₂-TPR, CO₂-TPD และ TGA ทดสอบประสิทธิภาพของตัวเร่งปฏิกิริยาด้วยปฏิกิริยาไฮโดรจิเนชันของคาร์บอนมอนอกไซด์ และ ปฏิกิริยาไฮโดรจิเนชันของคาร์บอนไดออกไซด์ที่อุณหภูมิ 250 องศาเซลเซียส ความดันบรรยากาศ จากผลการทดสอบพบว่า ตัวเร่งปฏิกิริยาCZA-3.5 มีประสิทธิภาพในการเร่งปฏิกิริยาได้ดีที่สุด เนื่องจากมีปริมาณ คอปเปอร์มาก ส่งผลให้มีพื้นที่ผิวของตัวเร่งปฏิกิริยา, ตำแหน่งที่ว่างไว และปริมาณของตำแหน่งกรดแก่เพิ่มขึ้น นอกจากนี้ยังมีการศึกษาผลของความแตกต่างของตัวปรับปรุงเช่น Zr และ Mn จากการทดลองเห็นได้ชัดว่า การปรับปรุงตัวเร่งปฏิกิริยาด้วยMnช่วยให้พื้นที่ผิวของตัวเร่งปฏิกิริยา, ตำแหน่งที่ว่างไว และปริมาณของตำแหน่งกรดแก่เพิ่มขึ้น และยังช่วยลดขนาดผลึกของCuOอีกด้วย ตัวเร่งปฏิกิริยาที่ปรับปรุงด้วยMnจึงมีประสิทธิภาพสูงสุดสำหรับปฏิกิริยาไฮโดรจิเนชันของคาร์บอนไดออกไซด์ ส่วนตัวเร่งปฏิกิริยาที่ปรับปรุงด้วยZrจะมีประสิทธิภาพสูง เมื่อทดสอบปฏิกิริยาด้วยคาร์บอนมอนอกไซด์ไฮโดรจิเนชัน ในส่วนสุดท้ายค่าความคงตัวของตัวเร่งปฏิกิริยา CZA-2, CZ-Zr-2 และ CZ-Mn-2 จะถูกตรวจสอบความแตกต่างระหว่างตัวเร่งปฏิกิริยาที่ยังไม่ถูกใช้งานและตัวเร่งปฏิกิริยาหลังการใช้งานแล้ว 5 ชั่วโมง เพื่อหาสาเหตุของการเสื่อมสภาพของตัวเร่งปฏิกิริยา

สาขาวิชา วิศวกรรมเคมี

ปีการศึกษา 2563

ลายมือชื่อนิสิต

ลายมือชื่อ อ.ที่ปรึกษาหลัก

6170463121 : MAJOR CHEMICAL ENGINEERING

KEYWORD: methanol synthesis; hydrogenation; Cu/ZnO/Al₂O₃; Manganese

Phapatchaya Phonrat : Effect of Cu/Zn ratios and Zr, Mn promoters on CuO/ZnO-based catalysts for methanol synthesis via hydrogenation of CO and CO₂. Advisor: Prof. BUNJERD JONGSOMJIT, Ph.D.

The aim of this research is to investigate CuO/ZnO/Al₂O₃ (CZA) catalysts with different Cu/Zn weight ratios including CZA-0.5, CZA-1, CZA-2 and CZA-3.5 catalysts having Cu/Zn weight ratios is 0.5, 1, 2 and 3.5, respectively. Catalysts were prepared by the co-precipitation method. Catalysts were characterized to determine the physical and chemical properties using various techniques such as N₂ adsorption, CO-Chemisorption, SEM-EDX, ICP-MS, XRD, XPS, H₂-TPR, CO₂-TPD and TGA. The catalysts were tested in CO hydrogenation and CO₂ hydrogenation at 250 °C under atmospheric pressure. From reaction test, it was found that CZA-3.5 catalyst exhibited the highest catalytic activity due to the highest copper contents resulting in increasing surface area, metallic copper surface and number of strong basic sites. In addition, effect of Zr and Mn promoters was also investigated. The results presented that Mn promoter can increase the surface area, metallic copper surface, copper dispersion, number of strong basic sites, but decrease crystallite size of CuO. The CZ-Mn-2 catalyst had the highest catalytic activity for CO₂ hydrogenation. Meanwhile, the CZ-Zr-2 catalyst exhibited the highest catalytic activity for CO hydrogenation. In the final part, the stability of CZA-2, CZ-Zr-2 and CZ-Mn-2 catalysts was investigated to determine the differences between the fresh and spent catalysts for comprehend cause of catalyst deactivation.

Field of Study: Chemical Engineering

Student's Signature

Academic Year: 2020

Advisor's Signature

ACKNOWLEDGEMENTS

First and foremost, I am extremely grateful to my research supervisor, Professor Dr. Bunjerd Jongsomjit for supporting of knowledge and providing precious guidance throughout the course of this research. I am most grateful for teaching and advice, not only the research methodologies but also many other methodologies in life.

Additionally, I am extremely thankful to my committee: Associate Professor Dr. Pattaraporn Kim (Chairman), Professor Dr. Joongjai Panpranot (Examiner) and Assistant Professor Dr. Sasiradee Jantasee (External Examiner) for suggestions of this research and the Malaysia Thailand Joint Authority (MTJA) project that supported me for doing this research.

Finally, I would like to thank all staffs of the Center of Excellence on Catalysis and Catalytic Reaction Engineering, Chulalongkorn University and my friends with great supports throughout the period of this research.

Phapatchaya Phonrat

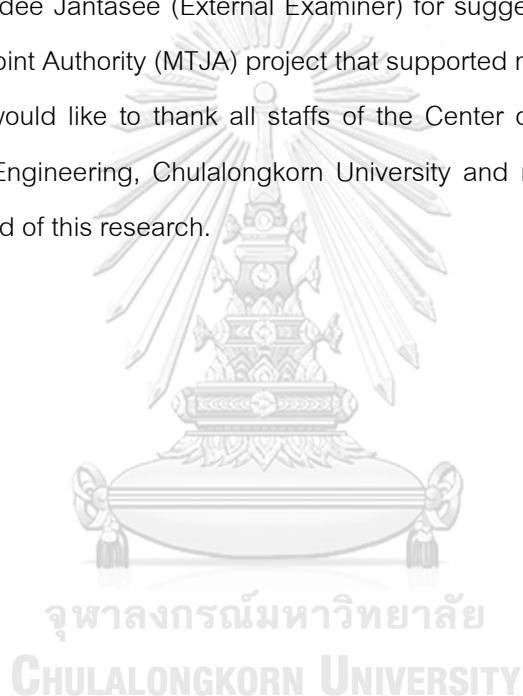


TABLE OF CONTENTS

	Page
.....	iii
ABSTRACT (THAI).....	iii
.....	iv
ABSTRACT (ENGLISH)	iv
ACKNOWLEDGEMENTS.....	v
TABLE OF CONTENTS.....	vi
LIST OF TABLES.....	ix
LIST OF FIGURES	x
INTRODUCTION.....	1
1.1 Background.....	1
1.2 Research objectives	3
1.3 Research scopes.....	3
1.4 Research methodology.....	5
1.5 Research plan.....	7
BACKGROUND AND LITERATURE REVIEW.....	8
2.1 Methanol.....	8
2.2 The reaction mechanism of methanol synthesis (on the catalyst surface)	9
2.3 CuO/ZnO/Al ₂ O ₃	10
2.4 Zirconium dioxide	11
2.5 Manganese (II) oxide	11
2.7 Literature reviews	13

EXPERIMENT	28
3.1 Catalysts characterizations	28
3.1.1. Chemicals for catalyst preparation	28
3.1.2. Preparation of CZA catalysts	28
3.2 Catalyst characterization	29
3.2.1. Scanning electron microscopy (SEM)	29
3.2.2. Energy dispersive X-ray spectroscopy (EDX)	29
3.2.3 Inductively coupled plasma mass spectrometry (ICP-MS)	29
3.2.4. X-ray diffraction (XRD).....	29
3.2.5. N ₂ physisorption	30
3.2.6. CO-Chemisorption (CO-Chem).....	30
3.2.8. Temperature-programmed reduction (TPR)	31
3.2.9. Temperature-programmed desorption of carbon dioxide (CO ₂ -TPD)	31
3.3 Reaction test	31
RESULTS AND DISCUSSION	34
4.1. Effect of Cu/Zn weight ratios in CZA catalysts.	34
4.1.1. Catalyst characterization.....	34
4.1.2 Catalyst performance	43
4.2. Effect of ZrO ₂ and MnO promoters.	45
4.2.1. Catalyst characterization.....	45
4.2.2 Catalyst performance	52
4.3. The deactivation of catalysts	54
CONCLUSIONS AND RECOMMENDATIONS	57

REFERENCES.....69

VITA76



จุฬาลงกรณ์มหาวิทยาลัย
CHULALONGKORN UNIVERSITY

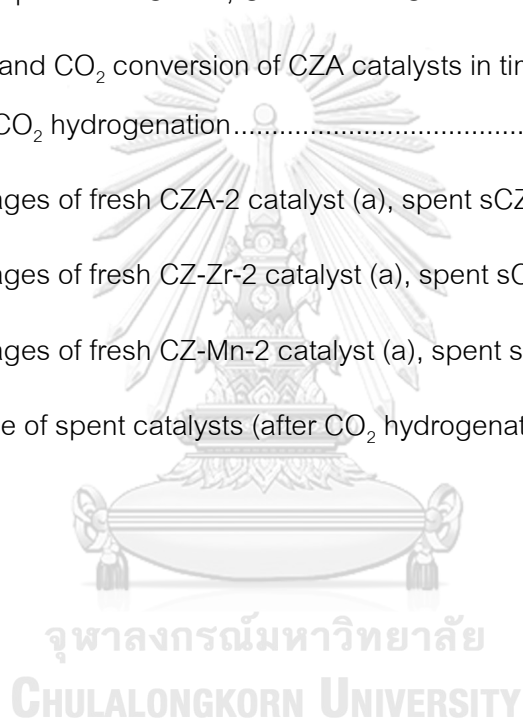
LIST OF TABLES

	Page
Table 1. The chemical ratio of prepared catalysts	3
Table 2. Properties of methanol	8
Table 3. The CuO/ZnO/Al ₂ O ₃ catalysts in Manufacturer	10
Table 4. Properties of Zirconium nitrate	11
Table 5. Properties of Manganese nitrate	12
Table 6. The conditions and significant review	14
Table 7. The chemicals used in the catalyst preparation	28
Table 8. Condition of TCD detector	32
Table 9. Condition of FID detector	33
Table 10. Element distribution of different CZA catalysts	37
Table 11. Textural properties of different CZA catalysts	38
Table 12. The amounts of basic sites of all CZA catalysts	43
Table 13. Catalyst activity of CZA catalysts	44
Table 14. Element distribution of CZA-2, CZ-Zr-2 and CZ-Mn-2 catalysts.	46
Table 15. Textural properties of CZA-2, CZ-Zr-2 and CZ-Mn-2 catalysts	48
Table 16. The amounts of basic sites of CZA-2, CZ-Zr-2 and CZ-Mn-2 catalysts	52
Table 17. Catalyst activity of CZA-2, CZ-Zr-2 and CZ-Mn-2 catalysts	53
Table 18. EDX elemental analysis on spent catalysts	55

LIST OF FIGURES

	Page
Figure 1. The methanol importation and exportation of Thailand.....	2
Figure 2. Molecular structure of methanol	8
Figure 3. The application of methanol	9
Figure 4. Reaction mechanisms for methanol synthesis via CO and CO ₂ hydrogenation.	10
Figure 5. XRD patterns of different Cu/Zn/Al catalysts (•) CuO, (Δ) ZnO, (○) Zincian malachite, (Cu,Zn) ₂ (OH) ₂ CO ₃	25
Figure 6. reaction pathway of CO ₂ hydrogenation	26
Figure 7. CO ₂ adsorbed species over weak, medium and strong basic sites.....	27
Figure 8. The Schematic of methanol synthesis and gas chromatography system	32
Figure 9. The SEM-EDX images of CZA-0.5 catalyst.....	34
Figure 10. The SEM-EDX images of CZA-1 catalyst.....	35
Figure 11. The SEM-EDX images of CZA-2 catalyst.....	35
Figure 12. The SEM-EDX images of CZA-3.5 catalyst.....	36
Figure 13. XRD pattern of different CZA catalysts.....	38
Figure 14. The XPS spectra of all CZA catalysts. (a) The XPS spectra of Cu species, b) The XPS spectra species and c) The XPS spectra of Al species	40
Figure 15. H ₂ -TPR profiles of all CZA catalysts.....	41
Figure 16. CO ₂ -TPD profiles of all CZA catalysts.....	42
Figure 17. The CO and CO ₂ conversion of CZA catalysts in time on stream 5 h. (a) CO hydrogenation (b) CO ₂ hydrogenation.....	44
Figure 18. The SEM-EDX images of CZ-Zr-2 catalyst.	45

Figure 19. The SEM-EDX images of CZ-Mn-2 catalyst.....	46
Figure 20. XRD pattern of CZA-2, CZ-Zr-2 and CZ-Mn-2 catalysts.	47
Figure 21. The XPS spectra of CZA-2, CZ-Zr-2 and CZ-Mn-2 catalysts. (a) The XPS spectra of Cu species, b) The XPS spectra of Zn species, c) The XPS spectra of Zr species and d) The XPS spectra of Mn species.....	49
Figure 22. H ₂ -TPR profiles of CZA-2, CZ-Zr-2 and CZ-Mn-2 catalysts.....	50
Figure 23. CO ₂ -TPD profiles of CZA-2, CZ-Zr-2 and CZ-Mn-2 catalysts.....	51
Figure 24. The CO and CO ₂ conversion of CZA catalysts in time on stream 5 h. (a) CO hydrogenation (b) CO ₂ hydrogenation.....	54
Figure 25. SEM images of fresh CZA-2 catalyst (a), spent sCZA-2 catalyst (b).....	54
Figure 26. SEM images of fresh CZ-Zr-2 catalyst (a), spent sCZ-Zr-2 catalyst (b)	55
Figure 27. SEM images of fresh CZ-Mn-2 catalyst (a), spent sCZ-Mn-2 catalyst (b)	55
Figure 28. TG profile of spent catalysts (after CO ₂ hydrogenation for 5 h).....	56



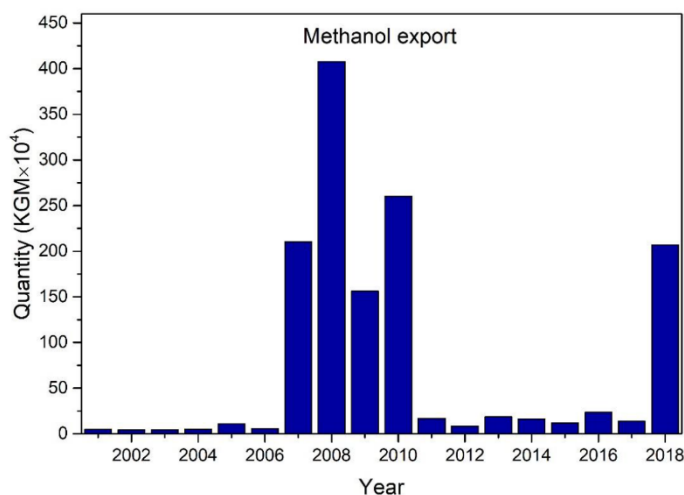
CHAPTER 1

INTRODUCTION

1.1 Background

Energy is necessary for the development of science and technology. At present, fossil fuels have been major source of energy. Unfortunately, fossil fuels are non-renewable energy. Thailand is another country that has the rate of energy consumption rises up every year. When the demand of energy has increased causing fossil fuels has decreased. Therefore, it is necessary to find a new energy source to substitute the fossil fuel. Synthetic fuel is new energy source such as methanol, ethanol, dimethyl ether (DME) and hydrogen. Presently, the main competitors appear to be methanol and hydrogen. Although hydrogen has higher energy content than methanol [1], it has the costs of purification processes and the difficulties for storage and transport [2].

Methanol is an important feedstock of many chemical industries such as formaldehyde, methyl tert-butyl ether (MTBE), acetic acid, methyl methacrylate (MMA), methylamines and dimethyl ether (DME). Besides chemical feedstock, methanol is used as fuel and a building block. Each day approximately 100,000 tons of methanol is used. In Thailand during the years 2017 and 2018, the methanol importation tended to increase showing the increasing of demand of methanol. On the other hand, the methanol exportation has low quantity production. The methanol importation and exportation of Thailand is shown in Figure 1.



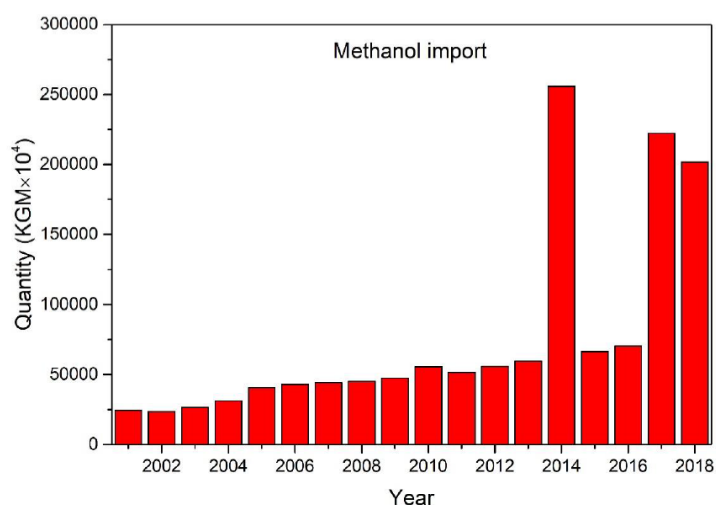


Figure 1. The methanol importation and exportation of Thailand

Industrially, methanol is mainly produced from CO hydrogenation at 200-300 °C under pressure of 3.5-10 MPa. Nevertheless, methanol synthesis from CO₂ hydrogenation is being the interesting process at the moment. CO₂ hydrogenation is approached to reduce CO₂ in the atmosphere. It is well known that CO₂ is the main environmental pollution for global warming.

Copper-based catalysts have been used in methanol synthesis for more than 45 years, although the nature of the active site is still not fully understood. The CuO/ZnO/Al₂O₃ is the main catalyst for industrial methanol synthesis. In fact, CuO/ZnO/Al₂O₃ has been reported as the most active catalyst for methanol synthesis via CO hydrogenation. On the other hand, CuO/ZnO/Al₂O₃ catalyst is not the best for methanol synthesis via CO₂ hydrogenation [3, 4]. Water is a byproduct from methanol synthesis via CO₂ hydrogenation, which is the negative effect on the rate of methanol formation of Al₂O₃ [4]. In the above problem, it leads to improvement of the catalyst by other promoters. The other promoters such as ZrO₂, MnO, Cr₂O₃, SiO₂, Ga₂O₃, etc. were studied.

This research is divided into two parts. Firstly, the CuO/ZnO/Al₂O₃ catalysts with different amounts of copper loading was synthesized. Then, CuO/ZnO/Al₂O₃ catalysts was tested in methanol synthesis via CO hydrogenation and CO₂ hydrogenation at 250 °C under atmospheric pressure for 5 hours. Secondly, the effect of ZrO₂ and MnO promoters was further studied. Furthermore, the prepared catalysts were characterized by SEM, EDX, ICP-MS, XRD, N₂ physisorption, CO-chemisorption, XPS, H₂-TPR and CO₂-TPD.

1.2 Research objectives

The aim of this research is to investigate CuO/ZnO/Al₂O₃ catalysts with different amounts of copper content in methanol synthesis and their catalytic properties via CO and CO₂ hydrogenation. Furthermore, this research also investigates the effect of ZrO₂ and MnO promoters.

1.3 Research scopes

1.3.1. Catalyst preparation

1.3.1.1. Preparation of CuO/ZnO/Al₂O₃ catalysts (CZA) by co-precipitation method with Al₂O₃ (10 wt.%) and different weight ratios of Cu/Zn. The chemical ratios of prepared catalysts are shown in **Table 1**.

Table 1. The chemical ratio of prepared catalysts

Catalyst	Cu/Zn/Al (wt.%)	Cu/Zn (wt.%)
CZA-0.5	30/60/10	0.5
CZA-1	45/45/10	1
CZA-2	60/30/10	2
CZA-3.5	70/20/10	3.5

1.3.1.2. Preparation of CuO/ZnO/ZrO₂ and CuO/ZnO/MnO catalysts by coprecipitation method with ratio of Cu:Zn:Zr and Cu:Zn:Mn = 60:30:10 wt.%. CZ-Zr-2 and CZ-Mn-2 instead of CuO/ZnO/ZrO₂ and CuO/ZnO/MnO, respectively.

1.3.2. Characterization of catalyst

- 1.3.2.1. Scanning electron microscopy (SEM)
- 1.3.2.2. Energy dispersive X-ray spectroscopy (EDX)
- 1.3.2.3. Inductively coupled plasma mass spectrometry (ICP-MS)
- 1.3.2.4. X-ray diffraction (XRD)
- 1.3.2.5. N₂ physisorption
- 1.3.2.6. CO-Chemisorption (CO-Chem)
- 1.3.2.7. X-ray photoelectron spectroscopy (XPS)
- 1.3.2.8. Temperature-programmed reduction (TPR)

1.3.2.9. Temperature-programmed desorption of carbon dioxide (CO₂-TPD)

1.3.2.10. Thermal gravimetric analysis (TGA)

1.3.3. Activity test

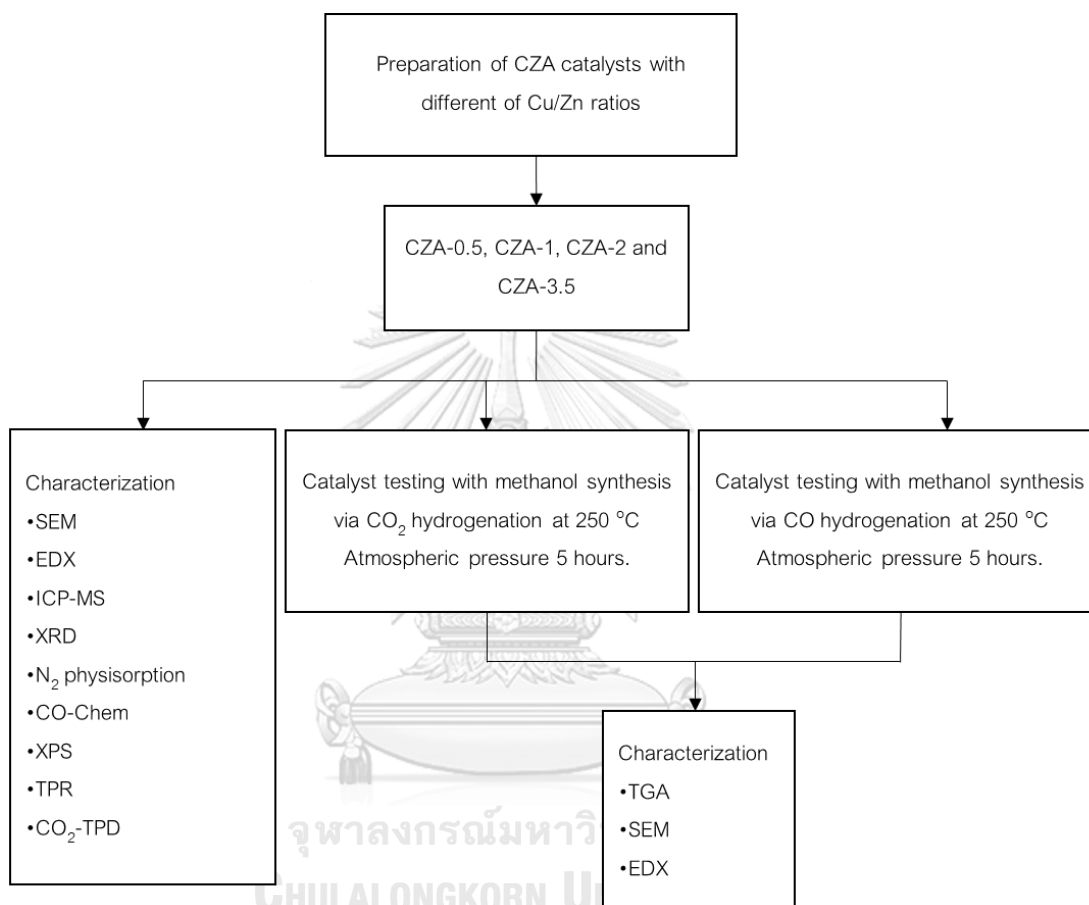
1.3.3.1. Testing the activity of catalysts in CO hydrogenation at 250 °C under atmospheric pressure, feeding reactants of CO:H₂ = 1:2 for 5 hours.

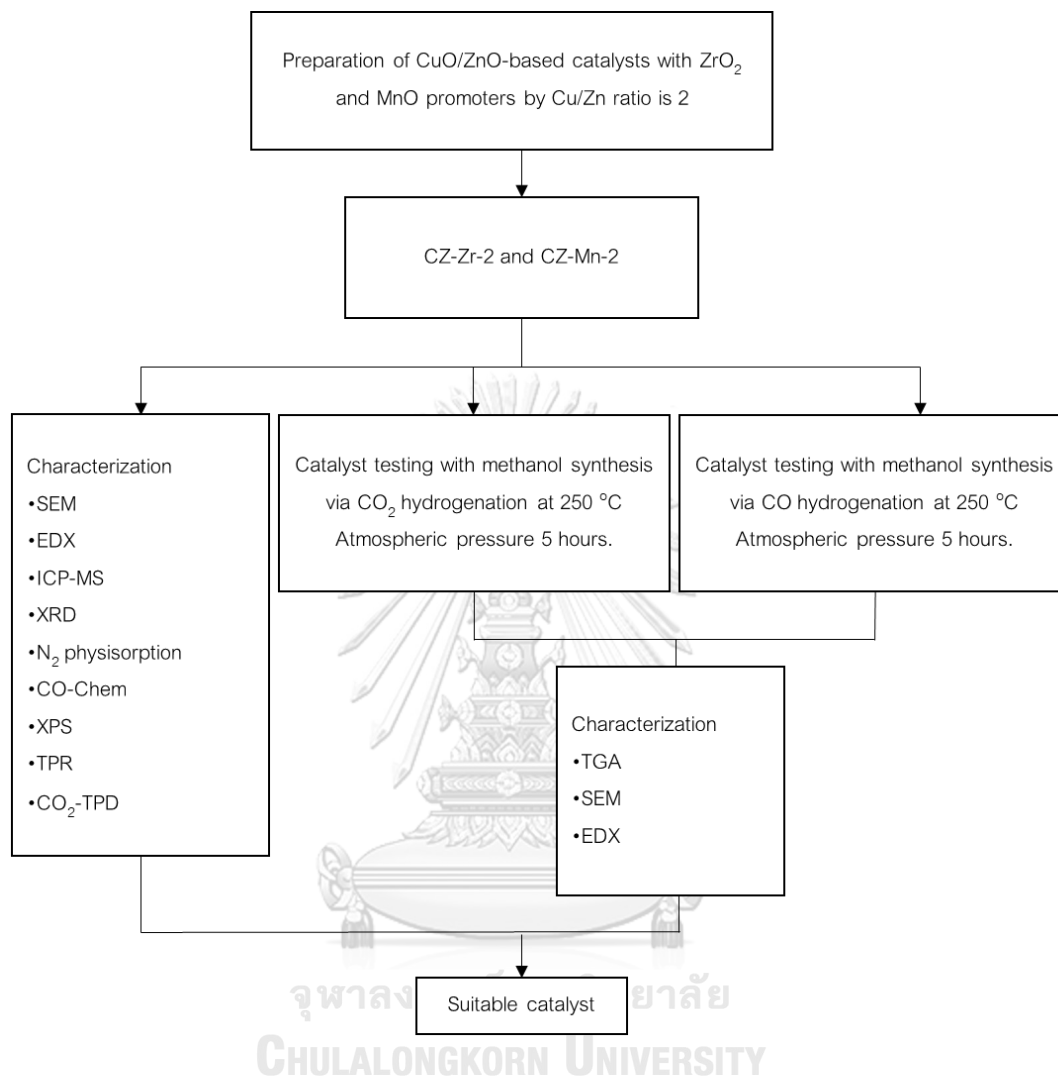
1.3.3.2. Testing the activity of catalysts in CO₂ hydrogenation at 250 °C under atmospheric pressure, feeding reactants of CO₂:H₂ = 1:3 for 5 hours.



1.4 Research methodology

Part 1: Methanol synthesis from CO hydrogenation and CO₂ hydrogenation using different Cu/Zn ratios in CZA catalysts



Part 2: The effect of ZrO_2 and MnO promoters

CHAPTER 2

BACKGROUND AND LITERATURE REVIEW

2.1 Methanol

Methanol is the primary alcohol which is the simplest alcohol. The chemical formula of methanol is CH_3OH that its molecular structure is a linkage between a methyl group and a hydroxyl group is shown in Figure 2. Methanol is a polar liquid at room temperature, colorless, volatile, flammable and pungent odor like ethyl alcohol. The other names of methanol are methyl alcohol, methyl hydrate, methyl hydroxide, wood spirit and wood alcohol. The specific physical and chemical properties of methanol are shown in Table 1 [5, 6].

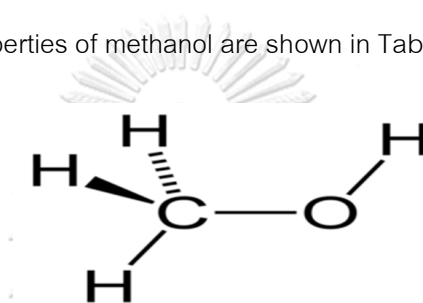


Figure 2. Molecular structure of methanol

Table 2. Properties of methanol

Properties	Information
Molecular weight	32.04 g/mol
Density	0.792 g/cm ³
Boiling Point	64.70 °C
Melting Point	-97.60 °C
Vapor pressure	13.02 kPa (at 20 °C)
Appearance	Colorless liquid

Methanol is used as the main feedstock for the production of many chemicals. The applications of methanol are very different as shown in figure 3 [7]. Approximately 30% of methanol production is converted into formaldehyde. Other chemicals such as acetic acid, dimethyl terephthalate, methyl chloride, methyl methacrylate, methyl tert-butyl ether (MTBE), tert-amyl methyl ether (TAME), dimethyl ether (DME) and olefins can be produced from methanol.

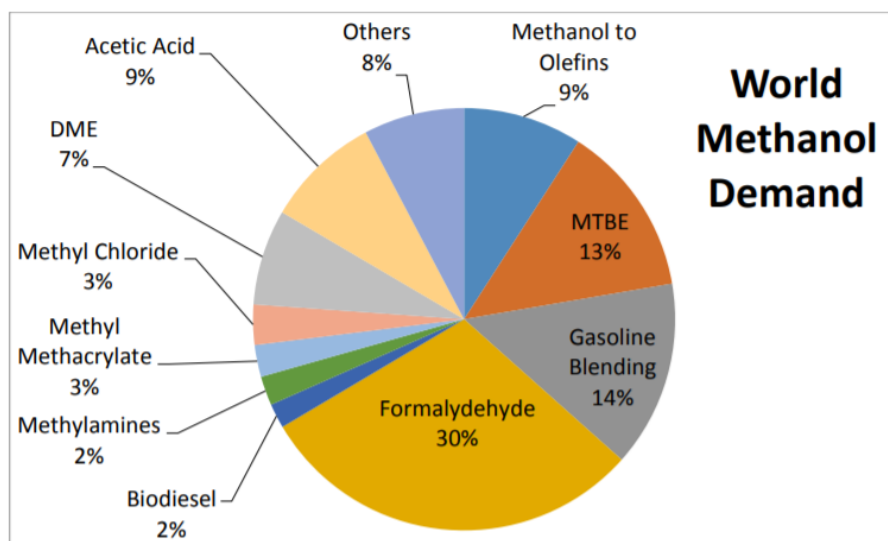


Figure 3. The application of methanol

2.2 The reaction mechanism of methanol synthesis (on the catalyst surface)

Three major reactions are possible in the methanol synthesis including: (1) CO hydrogenation, (2) CO₂ hydrogenation and (3) the reverse water gas shift (RWGS) reaction.



Both the methanol synthesis via CO hydrogenation and the methanol synthesis via CO₂ hydrogenation is exothermic process. Accordingly, the equilibrium yield of methanol decreases with increasing temperature. The reverse water gas shift (RWGS) reaction is the side reaction for methanol synthesis via CO₂ hydrogenation which is endothermic reaction. Therefore, the methanol synthesis via CO₂ hydrogenation should not operate at high temperature.

The mechanism of methanol synthesis via CO hydrogenation and CO₂ hydrogenation [8] is shown in Figure 4. Three common pathways for methanol synthesis include the formate pathway, the formyl pathway and carboxyl pathway. The formate pathway is pathway for direct

conversion of CO_2 to methanol and the formyl pathway is pathway for conversion of CO to methanol. The water gas shift mechanism undergoes through a carboxyl intermediate.

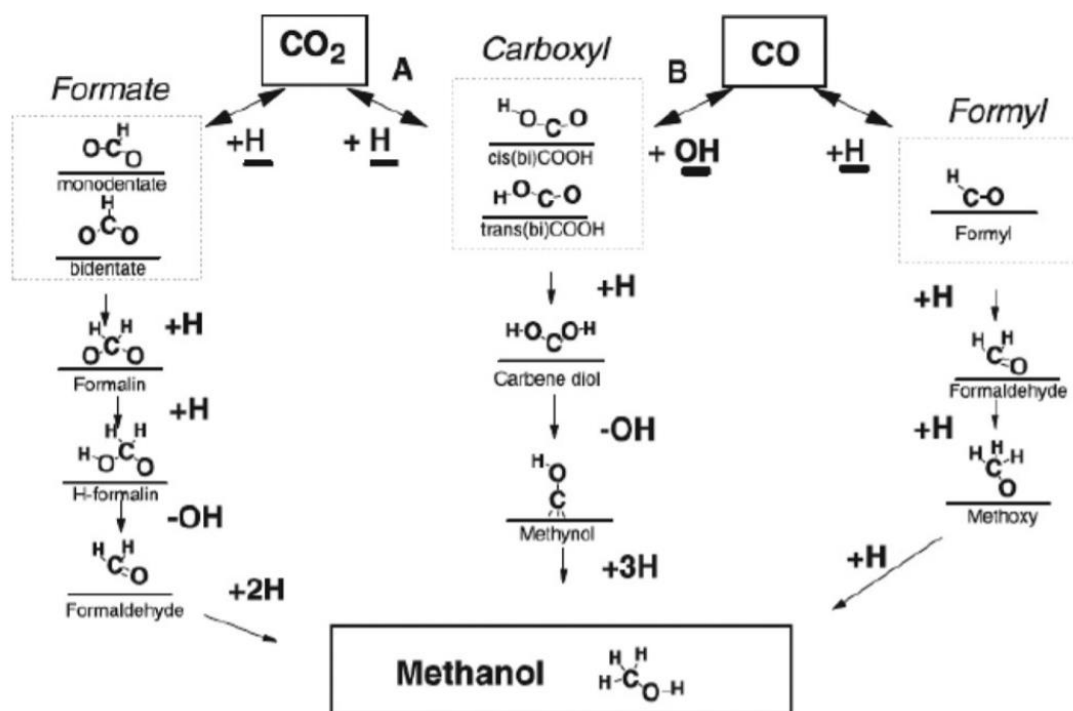


Figure 4. Reaction mechanisms for methanol synthesis via CO and CO_2 hydrogenation.

2.3 $\text{CuO}/\text{ZnO}/\text{Al}_2\text{O}_3$

Normally, heterogeneous catalysts consist of three major parts including active site, support and promoter. The Cu-based catalyst was the main used in methanol synthesis. Cu is the active metal, whereas ZnO acts as supporter that is increases the stabilization and dispersion of copper. In addition, Al_2O_3 is a promoter that improves the thermostability and activity of copper-based catalyst.

The $\text{CuO}/\text{ZnO}/\text{Al}_2\text{O}_3$ is the popular commercial catalyst for industrial methanol synthesis. The $\text{CuO}/\text{ZnO}/\text{Al}_2\text{O}_3$ catalysts in Manufacturer are shown in Table 2.

Table 3. The $\text{CuO}/\text{ZnO}/\text{Al}_2\text{O}_3$ catalysts in Manufacturer

Manufacturer	Cu	Zn	Al	Reference
BASF K3-110	40	40	20	[9]
ICI	20 - 35	15 - 50	4 - 20	[10]

IFP	45 - 70	15 - 35	4 - 20	[10]
Dupont	50	19	31	[10]
Lurgi	60 - 70	20 - 30	5 - 15	[10]
ICI 51-2	62	35	3	[11]
Sud Chemie	65	22	12	[12]
Alfa Aesar-Johnson Matthey	50.6	22.5	4.6	[13]
Alfa Aesar- HiFUEL R120	50	25	25	[14]

2.4 Zirconium dioxide

Zirconium dioxide (ZrO_2) or zirconia is the oxide form of Zr. ZrO_2 acts as a promoter in methanol synthesis. Nowadays, ZrO_2 Zirconia has attracted much interest because it demonstrates a high activity for both CO hydrogenation and CO_2 hydrogenation. Additionally, ZrO_2 is increase the dispersion of copper, reduce crystalline site, increase the basicity, increase activity and not sensitive to water. The precursor for ZrO_2 preparation is Zirconium nitrate.

Table 4. Properties of Zirconium nitrate

Properties	Information
Chemical formula	$Zr(NO_3)_4$
Molecular weight	339.244 g/mol
Density	1.415 g/cm ³ at 20 °C
Melting point	-
Boiling point	decompose 100 °C
Appearance	White powder crystal

2.5 Manganese (II) oxide

The metal oxide form of Mn is MnO , which is mainly used as promoter of catalyst. To avoid unwanted byproducts such as dimethyl ether (DME), the catalyst should not have acid

properties. In fact, MnO shows the increase in basicity of catalyst. The methanol selectivity relatively increases with basic site of catalyst. The precursor for MnO preparation is manganese nitrate.

Table 5. Properties of Manganese nitrate

Properties	Information
Chemical formula	Mn(NO ₃) ₂
Molecular weight	178.95 g/mol
Density	1.536 g/cm ³
Melting point	37 °C
Boiling point	100 °C
Appearance	White powder

2.6 Deactivation mechanism

Catalyst deactivation is a main problem in industry. Which catalyst deactivation induce to decreasing conversion and selectivity with time. As known, there are three fundamental reasons for catalyst deactivation including Poisoning, Coking or fouling and Sintering or phase transformation.

2.6.1. Deactivation of catalyst by Sintering

Loss of catalytic activity due to a loss of activity surface area.

- Crystal agglomeration and growth of the metals deposited on the support.
- Loss pore or structure of catalyst support.
- Change in the surface structure due to recrystallization, formation or elimination of surface defects.

2.6.2. Deactivation of catalyst by Coking or Fouling

This mechanism of formation is common to reactions involving hydrocarbon or side reaction leading to the formation of carbonaceous material being deposited on surface of catalyst. When the catalyst is already fouled or coked, the material is normally called spent catalyst.

The coke formation was identified into three reaction as following, (1) The Boudouard reaction, (2) Reduction of CO, (3) Methane cracking.



As know, the types of coke divided into two groups according to the range of temperature including amorphous coke and graphitic carbon.

2.6.3. Deactivation of catalyst by Poisoning

The loss of activity due to the strong chemisorption of impurities present in the feed stream on active sites of catalyst. This reduce the number of sites available for the main reaction.

2.7 Lirature reviews

This chapter reviewed the study on the copper-based catalysts for methanol synthesis via CO hydrogenation and CO₂ hydrogenation and also reviewed the suitable reaction condition for methanol synthesis via CO hydrogenation and CO₂ hydrogenation.

Table 6. The conditions and significant review

CO hydrogenation to methanol			
No	Catalyst, reactor type and reaction condition	Significant results	
1	<p>Catalyst Cu/M_{0.3}Zr_{0.7}O₂ catalyst (M=Ce, Mn, and Pr)</p> <ul style="list-style-type: none"> - Forced hydrolysis at low pH and deposition-precipitation. - Calcinated in air at 600 °C for 3 h. <p>Reactor type fixed-bed reactor</p> <p>Reaction condition at 250°C , 30 bars, H₂/CO = 3, total flow rate 60 cm³/min</p> <ul style="list-style-type: none"> - Reduced in H₂ at 300°C for 1 h. 	<ul style="list-style-type: none"> - The increase in methanol synthesis activity was paralleled by an increase in the hydrogen adsorption capacity of the catalyst and an increase in the fraction of Brønsted acidic bridging OH groups. - The highest methanol synthesis activity was observed for 3 wt% Cu/Ce_{0.3}Zr_{0.7}O₂. 	[15]
2	<p>Catalyst Cu/ZrO₂ catalysts</p> <ul style="list-style-type: none"> - Conventional precipitation method (CP) - Calcinated in air at 350 °C for 3 h. <p>Reactor type fixed-bed reactor</p> <p>Reaction condition at 300°C , 60 bars, 10,000 h⁻¹, H₂/CO = 2.</p> <ul style="list-style-type: none"> - Reduced in 20% H₂/N₂ at 260°C for 2 h. 	<ul style="list-style-type: none"> - Compared with ZrO₂-CP, ZrO₂-AN had larger specific surface area, cumulative pore volume and average pore size and showed relatively high CO conversion. - The increase in calcination temperatures led to the decrease in CO conversion. 	[16]

3	<p>Catalyst CuNi/SiO₂ catalyst</p> <ul style="list-style-type: none"> - Incipient wetness impregnation method - Drying and calcinating of ZrO(OH)₂ alcogel in N₂ (AN) - Calcinated on air for 4 h at 400°C. <p>Reactor type fixed-bed reactor</p> <p>Reaction condition Pressure 80 bars, temperature 220°C, GHSV 2000 h⁻¹, reactant mixture H₂:CO = 1</p> <ul style="list-style-type: none"> - reduced 20 vol.% H₂/N₂ at 300 °C pressure for 12-14 h. 	<ul style="list-style-type: none"> - Silica supported CuNi alloy catalyst highly active and selective catalysts for the hydrogenation of CO to form methanol. - No deactivation took place, but instead an activation process was observed during a total 73 h test of time on stream for the CuNi alloy catalyst. 	[17]
4	<p>Catalyst Cu/Zn/Al catalyst</p> <ul style="list-style-type: none"> - Co-precipitation. - Three samples molar content of 60:30:10, 45:45:10 and 33:33:33. - K promoted and substituting Zn and/or Al by Mn and/or Cr. - Calcination at 350 °C for 4 h. <p>Reactor type fixed-bed reactor</p> <p>Reaction condition at 300-320°C, 40 bars, W/F ratio of 0.74 g s/cm³, H₂/CO = 2.</p> <ul style="list-style-type: none"> - Reduced in H₂ flow at 350°C, 1 bar for 3 h. 	<ul style="list-style-type: none"> - Low Al component (K-Cu₄₅Zn₄₅Al₁₀) and Cu/Zn atomic ratio of 1:1 revealed the optimum performance in terms of selectivity and activity to produce higher alcohols. - The lower exposed copper surface that causes by large CuO crystals were formed as a result in reducing activity by 50% of replacement of Zn and/or Al by Mn and/or Cr. - The most perceptible changes were indicated for the catalyst, where a 50% increase in HAS was measured. 	[18]

5	<p>Catalyst Cu/ZnO/Al₂O₃ catalyst</p> <ul style="list-style-type: none"> - Co-precipitation. - Co-modified catalysts. - Calcination at 350 °C for 3 h. <p>Reactor type fixed-bed reactor</p> <p>Reaction condition at 280 °C, 60 bars, GHSV = 9600 h⁻¹, H₂/CO = 1</p> <ul style="list-style-type: none"> - Reduced in dilute H₂ (H₂/N₂ = 0.25), flow at 350 °C, 1 bar for 15 h. 	<ul style="list-style-type: none"> - An increasing of Cu/Co ratio that caused by the higher formation of alcohols and Cu/Co ratio 2.5 was recognized to optimum composition in term of activity and selectivity. - The distribution of product shifted favorably towards higher alcohols with increasing time on stream as an extended close interface contact between the metallic copper. 	[19]
6	<p>Catalyst Cu/Zn/Al/Zr</p> <ul style="list-style-type: none"> - Complete liquid-phase <p>Al/Zr atomic ratios of 4:1, 2:1</p> <ul style="list-style-type: none"> - Calcination at 300 °C for 8 h. <p>Reactor type a continuous-flow, slurry reactor</p> <p>Reaction condition at 250 °C, 45 bars</p> <ul style="list-style-type: none"> - Feed flowrate of 150mL/min. - Reduced in H₂/N₂ (75 mL/min, V(H₂)/ V(N₂) =1:4) flow at 280 °C, 1 bar for 8 h. 	<ul style="list-style-type: none"> - The increasing of Zr/Al atomic ratio, the catalytic performance and stability would be also increased. - Zr was useful to improve the stability of the catalysts. - For improving the dispersion of copper and made the catalyst easier to reduce. 	[20]

7	<p>Catalyst CuZnAlZr catalyst</p> <ul style="list-style-type: none"> - CZAZ co-precipitation. - CZAZ-S@SiO₂ sol-gel method - Calcination at 350°C for 3 h and 400°C for 3 h <p>Reactor type fixed-bed reactor</p> <p>Reaction condition at 250-280°C, 50 bars, GHSV = 4000 mL g_{cat}⁻¹h⁻¹, H₂/CO = 2</p> <ul style="list-style-type: none"> - Reduced at 250°C for 6 h with a 10 vol% H₂/N₂ under atmospheric pressure. 	<p>[21]</p> <ul style="list-style-type: none"> - The modification of CTAB can increase the BET surface area, pore volume and specific copper surface area of the catalyst. - Coating silica layer on CZAS can improve the stability of the catalyst for CO hydrogenation to methanol, but the CO conversion is withered apparently
---	---	--

CO ₂ hydrogenation to methanol			
No	Catalyst, reactor type and reaction condition	Significant results	Reference
1	<p>Catalyst Cu-Ti/γ-Al₂O₃ catalyst</p> <ul style="list-style-type: none"> - Conventional impregnation <p>Reactor type Fixed bed micro reactor</p> <p>Reaction condition Temperature 240°C, Pressure 30 bars, H₂/CO₂ = 3, GHSV = 3600 h⁻¹</p> <ul style="list-style-type: none"> - Reduced in H₂ at 300°C for 3 h - 2 mL catalyst 	<ul style="list-style-type: none"> - The addition of Ti to catalyst shows a higher conversion of CO₂ and higher yield of methanol. - The yield of methanol is in the order of Cu-Ti(10)/γAl₂O₃ > Cu-Ti(17)/γ-Al₂O₃ > Cu-Ti(5)/γ-Al₂O₃ > Cu/γ-Al₂O₃. - Cu-Ti(10)/γ-Al₂O₃ selectivity 13.5%, conversion 22.5% 	[22]
2	<p>Catalyst Cu/ZnO/Al₂O₃ catalyst</p> <ul style="list-style-type: none"> - Gel-network-coprecipitation (PCZA1X)(X= 1-5) - Conventional oxalate coprecipitation (PCZA2) - Conventional carbonate coprecipitation (PCZA3) <p>Reactor type Fixed bed micro reactor</p> <p>Reaction condition Temperature 240°C, Pressure 20 bars, H₂/CO₂ = 3, GHSV = 3600, 7200 h⁻¹</p>	<ul style="list-style-type: none"> - The Cu/ZnO/Al₂O₃ catalysts prepared by the oxalate gel-network-coprecipitation process exhibit a much higher activity and selectivity than prepared by conventional methods. - The catalytic CO₂ conversion on the conventional oxalate precipitated catalyst is higher than that on a conventional carbonate precipitated catalyst. 	[23]

3	<p>Catalyst Mg and Mn oxide additions Cu/ZnO/ZrO₂</p> <ul style="list-style-type: none"> - Decomposing the citrate complexes - Calcinated on air for 1 h at 100, 200, 250 and 300°C. <p>Reactor type fixed-bed reactor</p> <p>Reaction condition Pressure 80 bar, temperature 220°C, GHSV 5400 h⁻¹, reactant mixture H₂:CO₂ = 3</p> <ul style="list-style-type: none"> - reduced 10% H₂ in N₂ at 200 °C under atmospheric pressure for 15 h. 	<p>- The catalytic activity increase by CuZnZr < CuZnZrMg < CuZnZrMn.</p> <ul style="list-style-type: none"> - Dispersion of Cu determined with the XRD line broadening method and from the reactive adsorption of N₂O increasing. 	[24]
4	<p>Catalyst Zr–Cu/ZnO catalyst</p> <ul style="list-style-type: none"> - CuZnO co-precipitation - Zr–Cu/ZnO successive-precipitation <p>Reactor type Fixed bed stainless steel reactor</p> <p>Reaction condition at 210-270°C, Pressure 50 bars, H₂/CO₂ = 3, GHSV = 4000 h⁻¹</p> <ul style="list-style-type: none"> - Reduced in H₂/N₂ at 260°C for 6 h - 1 mL catalyst 	<ul style="list-style-type: none"> - Both CO₂ conversion and methanol selectivity for Zr–Cu/ZnO were higher than that for CuZnO. - The methanol selectivity decreased at high temperatures. - The methanol yield for Zr–Cu/ZnO catalyst reached maximum of 0.22 g mL⁻¹ h⁻¹ with the selectivity of 60.45% at about 250°C. 	[25]

5	<p>Catalyst Cu/Zn/Al/Zr catalyst</p> <ul style="list-style-type: none"> - Co-precipitation <p>Reactor type Fixed bed reactor</p> <p>Reaction condition Temperature 240°C, Pressure 40 bars, $H_2/CO_2 = 3$</p> <ul style="list-style-type: none"> - GHSV = 9742 h^{-1} - Reduced in H_2/N_2 at 240°C for 10 h 	<ul style="list-style-type: none"> - The catalyst preparation method. Both the activity and the methanol selectivity of CO_2 hydrogenation were improved. - 5 mole% Zr showed the best activity and thermal stability with a methanol STY that was 81% higher than a commercial industrial catalyst. 	[26]
6	<p>Catalyst Cu–ZnO/ZrO₂ catalyst</p> <ul style="list-style-type: none"> - Reverse co-precipitation under ultrasound irradiation <p>Reactor type Fixed bed micro reactor</p> <p>Reaction condition Temperature 200-240°C, Pressure 10-30 bars, $H_2/CO_2/N_2 = 9/3/1$</p> <ul style="list-style-type: none"> - GHSV = 4400 $NL\ h^{-1}\ kg_{cat}^{-1}$ - Reduced in H_2 at 300°C for 1 h - 0.5 g catalyst 	<ul style="list-style-type: none"> - At lower pressure, the conversion of CO_2 rising from 4 to 14%, counterbalanced by a drop in the CH_3OH selectivity from 63 to 17%. - Optimum Zn/Cu ratio = 0.3–0.5 	[4]

7	<p>Catalyst Cu/ZnO/ZrO₂ catalyst</p> <ul style="list-style-type: none"> - Urea–nitrate combustion <p>Reactor type Fixed bed reactor</p> <p>Reaction condition Temperature 240°C, Pressure 30 bars, H₂/CO₂ = 3, GHSV = 3600 h⁻¹</p> <ul style="list-style-type: none"> - Reduced in H₂/N₂ at 300°C for 3 h - 0.5 g catalyst 	<ul style="list-style-type: none"> - The CO₂ conversion increased with the decrease of urea amount and reached a maximum for sample 50-CZZ. - 50-CZZ catalyst selectivity 56.6%, conversion 17.0%, yield 9.6% - Methanol yield obtained over the catalyst prepared by combustion method lower than co-precipitation methods. 	[27]
8	<p>Catalyst Cu/Zn/Al/X catalyst (X = Mn, La, Ce, Zr and Y)</p> <ul style="list-style-type: none"> - Co-precipitation <p>Reactor type Fixed bed reactor</p> <p>Reaction condition Temperature 230-270°C, Pressure 50 bars, H₂/CO₂ = 3</p> <ul style="list-style-type: none"> - GHSV = 12,000 mL h⁻¹ g⁻¹ - Reduced in H₂ at 300°C for 8 h - 0.5 g catalyst 	<ul style="list-style-type: none"> - The introduction of modifier (Mn, La, Ce, Zr and Y) leads to higher BET specific surface area, Cu surface area and Cu dispersion. - The Y- and Zr-modified Cu/Zn/Al catalysts exhibit the highest CO₂ conversion and CH₃OH selectivity. 	[28]

9	<p>Catalyst CuO/ZnO/Al₂O₃</p> <ul style="list-style-type: none"> - Co-precipitation. - Graphene nanosheet (GNS) modified by high energy ball milling. - Calcination at 350 °C for 6 h. <p>Reactor type fixed bed microreactor.</p> <p>Reaction condition at 250°C, 30 bars, GHSV = 12000 h⁻¹</p> <ul style="list-style-type: none"> - Reactant gas H₂/CO₂/N₂ = 69:23:8. - Reduced in diluted H₂ (5% in N₂) flow at 280°C for 6 h. 	<ul style="list-style-type: none"> - With additional GNS into the CZA catalyst could enhance the catalyst performance for methanol production. - The 10 wt.% GNS modified CZA catalyst gave a STY of methanol 92.5% which higher than that on the CZA catalyst without GNS. 	[29]
10	<p>Catalyst CuO/ZnO/Al₂O₃</p> <p>Cu/Zn/Al atomic ratio 60/25/15</p> <ul style="list-style-type: none"> - Mechanical milling and combustion method - The pH 7.5–8.0. <p>Reactor type fixed-bed reactor</p> <p>Reaction condition at 240°C, 30 bars, 3600 h⁻¹, H₂/CO₂ = 3</p> <ul style="list-style-type: none"> - Reduced in H₂ flow at 270°C for 1 h 1 bar. 	<ul style="list-style-type: none"> - It is found that the combustion processes and physicochemical properties of catalysts depend strongly on the type and amount of fuel. - CZA-C-1.25 catalyst shows the highest catalytic activity for the hydrogenation of CO₂ to methanol. 	[30]

11	<p>Catalyst CuO/ZnO/Al₂O₃ catalyst</p> <ul style="list-style-type: none"> - Ammonia deposition-precipitation (ADP) method <p>Reactor type Fixed bed reactor</p> <p>Reaction condition at 220, 240 °C, Pressure 40 bars,</p> <p>H₂/CO₂/N₂ = 73/24/3</p> <ul style="list-style-type: none"> - WHSV = 1500 mL g_{cat}⁻¹h⁻¹ - Reduced in H₂ at 240 °C for 6 h - 0.7 g catalyst 	<ul style="list-style-type: none"> - The increasing of metal loading, the amount, size and thickness of layered particles increased markedly until they reached a maximum for the catalyst with Cu and ZnO loading of 33.61 wt. %. - The CO₂ conversion and yield of methanol increased gradually with the increase of the weight percentage of Cu and ZnO. 	[31]
12	<p>Catalyst Cu/ZnO/Al₂O₃</p> <ul style="list-style-type: none"> - Co-precipitation. - Calcination at 300 °C for 3 h. <p>Considered two conditions, namely washed and unwashed filtration.</p> <p>Reactor type fixed-bed reactor</p> <p>Reaction condition at 160-220 °C, 7 bars, GHSV = 1950 h⁻¹,</p> <p>H₂/CO₂ = 9:1</p>	<ul style="list-style-type: none"> - The unwashed method showed higher performance for methanol production than another method. - The lower precipitation temperature and unwashed by water was favorable for higher Copper dispersion, higher methanol synthesis activity and amorphous Cu crystal. 	[M7]

13	<p>Catalyst CuO/ZnO/Al₂O₃</p> <ul style="list-style-type: none"> - Co-precipitation. - Different In₂O₃ and Al₂O₃ contents. - Calcination at 320°C for 3 h. <p>Reactor type fixed-bed reactor</p> <p>Reaction condition at 250°C, 50 bars and GHSV = 15000 h⁻¹,</p> <p>H₂/CO₂ = 4</p> <ul style="list-style-type: none"> - Reduced in diluted H₂ (5% in N₂) flow at 295°C, 1 bar for 14 h. 	<ul style="list-style-type: none"> - The sample with higher amount of In₂O₃ exhibited higher stability. - The increasing of Pd into the catalyst could improve the methanol synthesis for CO₂ hydrogenation. 	[32]
14	<p>Catalyst CuO/ZnO/ZrO₂/Al₂O₃ catalyst</p> <ul style="list-style-type: none"> - Co-precipitation <p>Reactor type Fixed bed reactor</p> <p>Reaction condition at 220°C, Pressure 27.6 bars, H₂/CO₂ = 3, GHSV = 823 h⁻¹</p> <ul style="list-style-type: none"> - Reduced in H₂ at 250°C for 10 h - 0.5 g catalyst 	<ul style="list-style-type: none"> - Zr modified CZA catalysts were synthesized by the coprecipitation method. The effects of Al and Zr loading were investigated in both methanol and DME synthesis from CO₂ hydrogenation. - The optimized catalyst composition for methanol and DME synthesis was 4:2:1:0.5 for an atomic ratio of Cu/Zn/Zr/Al. 	[33]

Kamonlak Pongpanumaporn (2020) [34] studied the suitable pH in step of catalyst preparation. CuO/ZnO/Al₂O₃ catalyst was prepared by co-precipitation method with different pH including 7, 8 and 9. The result of this research showed that the pH 8 had the highest dispersion of CuO and high amount of basic site.

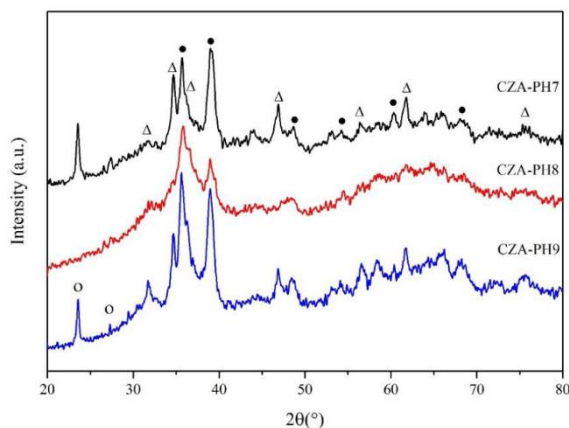


Figure 5. XRD patterns of different Cu/Zn/Al catalysts (•) CuO, (Δ) ZnO, (O) Zincian malachite, (Cu,Zn)₂(OH)₂CO₃.

Allam, D. et al. (2019) [35] studied the effect of the copper content. The CuO/ZnO/Al₂O₃ catalyst with different copper amounts in the range of 10-90 wt.% were tested in methanol synthesis from CO₂ hydrogenation. The results showed that The CuO/ZnO/Al₂O₃ catalyst with a Cu/Zn/Al weight ratio of 60/30/10 exhibited the highest CO₂ conversion and methanol selectivity. In addition, reaction was operated by varying pressure. The results showed that methanol selectivity increased with increasing the pressure because when reaction was operated at low pressure formate intermediate decomposed to CO better than the dioxomethylene formation.

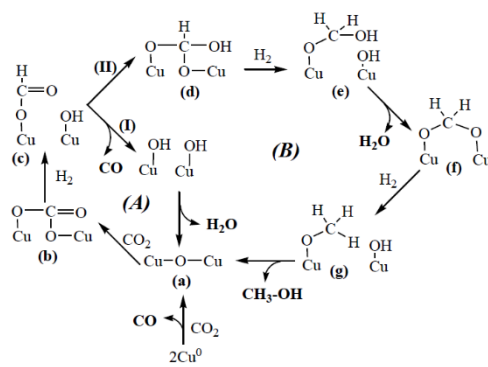
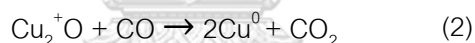
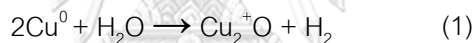


Figure 6. reaction pathway of CO₂ hydrogenation

Arena, F. et al. (2013) [36] investigated the effect of Al₂O₃, ZrO₂ and CeO₂ on Cu–ZnO catalyst. The catalysts were tested in methanol synthesis via CO₂ hydrogenation at 240°C under pressure of 5 MPa. In this research, the Cu–ZnO/ZrO₂ catalyst showed the best performance of all catalysts.

Lim, H. et al. (2009) [37] studied the effect of ZrO₂ on The CuO/ZnO/Al₂O₃ catalyst for methanol synthesis via CO hydrogenation at 240°C under pressure 5 MPa. The CuO/ZnO/Al₂O₃/ZrO₂ catalyst was compared with the CuO/ZnO/Al₂O₃ catalyst. The results showed that the CO conversion and methanol selectivity on CuO/ZnO/Al₂O₃/ZrO₂ catalyst were higher than CuO/ZnO/Al₂O₃ catalyst because smaller metallic copper particles and higher surface area.

Atake, I. et al. (2007) [38] studied the active sites on CuO/ZnO/Al₂O₃ catalysts as following reduction-oxidation between Cu⁰ to Cu⁺



Gao, P. et al. (2013) [28] studied the effect of Mn, La, Ce, Zr and Y promoter on The CuO/ZnO/Al₂O₃ catalyst for methanol synthesis via CO₂ hydrogenation at 240°C under pressure of 5 MPa. The results showed that,

- (1) Promoted of Mn, La, Ce, Zr and Y led to higher surface area and copper dispersion.
- (2) The Cu/Zn/Al/Y and Cu/Zn/Al/Zr catalysts exhibited the highest CO₂ conversion and methanol selectivity.

In addition, The CO₂-TPD was proposed three type of surface basic site on CZA catalysts including weak, moderate and strong. Which each basic site was explained by different CO₂ adsorbed species. It's was found that unidentate carbonates on strong basic site can be promote the methanol selectivity.

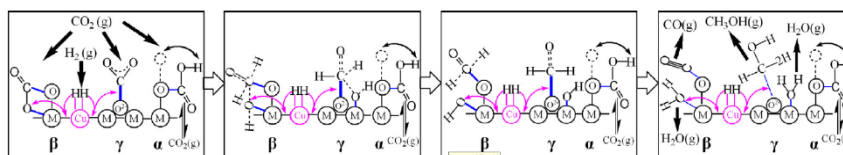
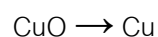
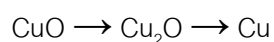


Figure 7. CO₂ adsorbed species over weak, medium and strong basic sites.

Li, C. et al. (2014) [39] investigated the reducibility of CuO by temperature-programmed reduction (TPR). The results showed that CuO was reduced at 250 °C by following;



Or



Meshkini, F. et al. (2010) [40] investigated the effect of metal oxide including Mn, Mg, Zr, Cr, Ba, W and Ce oxide modified the Cu/ZnO/Al₂O₃ catalyst. The results showed that Mn and Zr have the most increasing effect on catalytic activity. Addition of Zr can increase copper dispersion and area. Addition of Mn is accompanied by an increase in bulk and surface properties of the catalyst and easier reduction of CuO.

CHAPTER 3

EXPERIMENT

3.1 Catalysts characterizations

3.1.1. Chemicals for catalyst preparation

List of chemicals that were used in the catalyst preparation are shown in **Table 7**.

Table 7. The chemicals used in the catalyst preparation

Chemicals	Formula	Grade	Supplier
Aluminum nitrate nonahydrate	$\text{Al}(\text{NO}_3)_3 \cdot 9\text{H}_2\text{O}$	98%	Sigma- Aldrich
Copper (II) nitrate hemi(pentahydrate)	$\text{Cu}(\text{NO}_3)_2 \cdot 2.5\text{H}_2\text{O}$	98%	Sigma- Aldrich
Zinc nitrate hexahydrate	$\text{Zn}(\text{NO}_3)_2 \cdot 6\text{H}_2\text{O}$	98%	Sigma- Aldrich
Zirconium (IV) oxynitrate hydrate	$\text{ZrO}(\text{NO}_3)_2 \cdot x\text{H}_2\text{O}$	99%	Sigma- Aldrich
Manganese (II) nitrate tetrahydrate	$\text{Mn}(\text{NO}_3)_2 \cdot 4\text{H}_2\text{O}$	97%	Sigma- Aldrich

3.1.2. Preparation of CZA catalysts

Four CZA catalysts with different weight ratios of Cu/Zn were prepared by co-precipitation method including 10 wt.% of Al_2O_3 for all catalysts and weight ratios of Cu/Zn is 0.5, 1, 2 and 3.5 respectively. Firstly, the required amounts of nitrate precursors including $\text{Cu}(\text{NO}_3)_2 \cdot 2.5\text{H}_2\text{O}$, $\text{Zn}(\text{NO}_3)_2 \cdot 6\text{H}_2\text{O}$ and $\text{Al}(\text{NO}_3)_3 \cdot 9\text{H}_2\text{O}$ were dissolved in DI water (50 mL) at 80 °C. Then, the NaHCO_3 was slowly dropped in the precursor solution until the pH at 8. The solution mixture was stirred at 80 °C for 60 min and the metal complex precipitated. The mixture of precipitates was washed with DI water until neutral. The catalysts were dried at 110°C overnight and calcined in air at 350 °C for 3 h.

3.1.3. Preparation of CZ-Zr-2 and CZ-Mn-2 catalysts

The CZ-Zr-2 and CZ-Mn-2 catalysts were also prepared by co-precipitation method. The procedure for preparation catalyst is same as part 3.1.2., but $\text{ZrO}(\text{NO}_3)_2 \cdot x\text{H}_2\text{O}$ was used to replace $\text{Al}(\text{NO}_3)_3 \cdot 9\text{H}_2\text{O}$ for CZ-Zr-2 catalyst and $\text{Mn}(\text{NO}_3)_2 \cdot 4\text{H}_2\text{O}$ replaced $\text{Al}(\text{NO}_3)_3 \cdot 9\text{H}_2\text{O}$ for CZ-Mn-2 catalyst. The weight ratio of Cu:Zn:Zr and Cu:Zn:Mn is 60:30:10. After nitrate

precursors were dissolved in DI water (50 mL) at 80 °C, the NaHCO₃ was slowly dropped in the precursor solution until the pH at 8 was reached. The solution mixture was stirred at 80 °C for 60 min and the metal complex precipitated. The mixture of precipitates was washed with DI water until neutral. The catalysts were dried at 110°C overnight and calcined in air at 350 °C for 3 h.

3.2 Catalyst characterization

3.2.1. Scanning electron microscopy (SEM)

Scanning electron microscope (SEM) was used to investigate the morphology of the prepared catalyst. SEM observation with a JEOL mode JSM-6400.

3.2.2. Energy dispersive X-ray spectroscopy (EDX)

Energy dispersive X-ray spectroscopy (EDX) was used to investigate elemental dispersion on surface. EDX using Link Isis series 300 program.

3.2.3 Inductively coupled plasma mass spectrometry (ICP-MS)

Inductively coupled plasma mass spectrometry (ICP-MS) was used to determine elemental compositions in bulk catalyst including Cu, Zn, Al, Zr and Mn. Before analyzing in ICP-MS technique, the catalysts were dissolved with HCl.

3.2.4. X-ray diffraction (XRD)

X-ray diffraction (XRD) was used to analyze crystal structure and crystallite size. XRD patterns were recorded on a Bruker AXS Model D8 with Cu-K_α radiation ($\lambda = 0.15406$ nm) in the range $20^\circ < 2\theta < 80^\circ$. The crystallite size was calculated by using the Scherrer equation as follows:

$$D = \frac{K\lambda}{\beta \cos\theta}$$

Where K = unity constant factor

λ = X-ray wavelength

θ = the position of observe peak

β = X-ray diffraction broadening in half peak.

3.2.5. N₂ physisorption

N₂ physisorption was used to determine specific surface area by Brunauer-Emmett-Teller (BET) analysis. Furthermore, average pore size and pore volume were calculated from the method of Barrett-Joyner-Halenda (BJH). The hysteresis loop of catalysts was obtained using nitrogen gas adsorption at liquid nitrogen temperature (-196°C) in a Micromeritics ASAP 2000 automated system.

3.2.6. CO-Chemisorption (CO-Chem)

CO-Chemisorption was used to determine the number of surface-active sites and active sites dispersion. First, 0.05 g of catalyst was reduced by H₂ at 300 °C for 1 hour. Then, purging in the flow of He (25 mL/min) for 30 min. After this, Catalyst was cooled down to 30 °C and adsorbed by pulses of CO gas 80µL each time until catalyst was saturated. The number of surface-active sites and active sites dispersion can calculate by using equation as follows:

$$MSA_S = S_f \times \frac{V_{ads}}{V_g} \times \frac{100\%}{\%M} \times N_A \times \sigma_m \times \frac{m^2}{10^{18}nm^2}$$

Where MSA_S = surface-active sites

S_f = stoichiometry factor

V_{ads} = volume adsorbed, (cm³/g)

V_g = molar volume of gas at STP, 22414 (cm³/mol)

N_A = Avogadro's number, 6.023x10²³ (molecules/mol)

σ_m = cross-sectional area of active metal atom, (nm²)

$$D (\%) = S_f \times \frac{V_{ads}}{V_g} \times \frac{m. w.}{\%M} \times 100\%100\%$$

Where S_f = stoichiometry factor

V_{ads} = volume adsorbed, (cm³/g)

V_g = molar volume of gas at STP, 22414 (cm³/mol)

$m. w.$ = molecular weight of the metal, (a.m.u.)

$\%M$ = % metal, (%)

3.2.7. X-ray photoelectron spectroscopy (XPS)

X-ray photoelectron spectroscopy (XPS) was used to investigate the catalyst surface composition and oxidation state. The catalyst was determined in 0-1200 eV.

3.2.8. Temperature-programmed reduction (TPR)

The temperature-programmed reduction (TPR) is a powerful technique to determine the reduction behaviors of catalysts. 0.05 g of catalyst was pretreated by N_2 (25 mL/min) at 300 °C for 1 hour. Then catalyst was carried out 10% H_2/Ar with the heating rate 10 °C/min in the temperature range of 30 – 500 °C.

3.2.9. Temperature-programmed desorption of carbon dioxide (CO_2 -TPD)

Temperature-programmed desorption of carbon dioxide (CO_2 -TPD) was used to determine the basicity of catalyst. First, 0.05 g of catalyst was pretreated at 250 °C for 30 min. Then, catalyst was adsorbed by CO_2 (25 mL/min) at 30 °C in 1 hour. The desorption of CO_2 was carried out in He (25 mL/min) by increasing the temperature to 500 °C with the heating rate 10 °C/min.

3.2.10. Thermal gravimetric analysis (TGA)

Thermal gravimetric analysis (TGA) was used to determine the carbon deposition in the spent catalysts. TGA was carried out in TA Instruments SDT Q 600 analyzer. The 0.02 g catalyst was operated under flowing of air in the temperature range of 25 – 1000 °C with the heating rate 10 °C/min.

3.3 Reaction test

CO hydrogenation and CO_2 hydrogenation were carried out in fix-bed microreactor (O.D. 12 mm, height 50 cm), which is located in the electrical furnace. About 0.1 g of catalyst was packed into the reactor with quartz wool. Firstly, the catalyst was in situ pretreated by N_2 flow rate at 40 mL/min and 250 °C for 30 min under atmospheric pressure for removal of moisture and impurity. Then, the catalyst was reduced in a H_2 flow rate of 40 mL/min at 300 °C

for 1 h under atmospheric pressure. To start the reaction, the reactant was introduced into the reactor at 250 °C for 5 h under atmospheric pressure. The feed ratio is 1:2 by volume of CO:H₂ for CO hydrogenation and 1:3 by volume of CO₂:H₂ for CO₂ hydrogenation. The products were analyzed by a gas chromatograph (GC) with thermal conductivity detector (TCD) and flame ionization detector (FID). The operating condition of GC-2014 is shown in Tables 8 and 9.

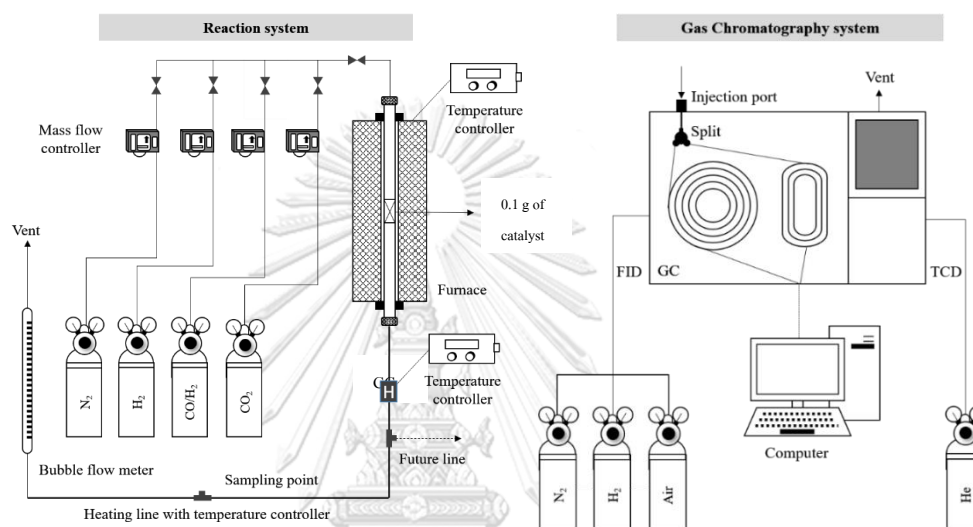


Figure 8. The Schematic of methanol synthesis and gas chromatography system

Table 8. Condition of TCD detector

Gas Chromatograph	Shimadzu GC 2014
GC type	Multi-detector
Detector 1	TCD
Pack-bed reactor	Shincarbon
Carrier gas	Herium gas
Injector temperature	170 °C
Column temperature	Initial 150 °C
(Link FID)	Hold 280 °C
	Cool down 150 °C
Detector temperature	150 °C

Time analysis 15 min

Table 9. Condition of FID detector

Gas Chromatograph	Shimadzu GC 2014
GC type	Multi-detector
Detector 1	FID
Pack-bed reactor	Rtx-5
Carrier gas	Nitrogen gas Hydrogen gas Air zero gas
Injector temperature	170 °C
Column temperature	Initial 150 °C
(Link FID)	Hold 280 °C Cool down 150 °C
Detector temperature	150 °C

CHAPTER 4

RESULTS AND DISCUSSION

This chapter shows the results of catalyst characterization and catalyst performance. This chapter is divided into 3 sections including 4.1 effect of Cu/Zn weight ratios in CZA catalysts, 4.2 effect of ZrO_2 and MnO promoters and 4.3 the deactivation of spent catalysts. Details of each section are as follows:

4.1. Effect of Cu/Zn weight ratios in CZA catalysts.

4.1.1. Catalyst characterization

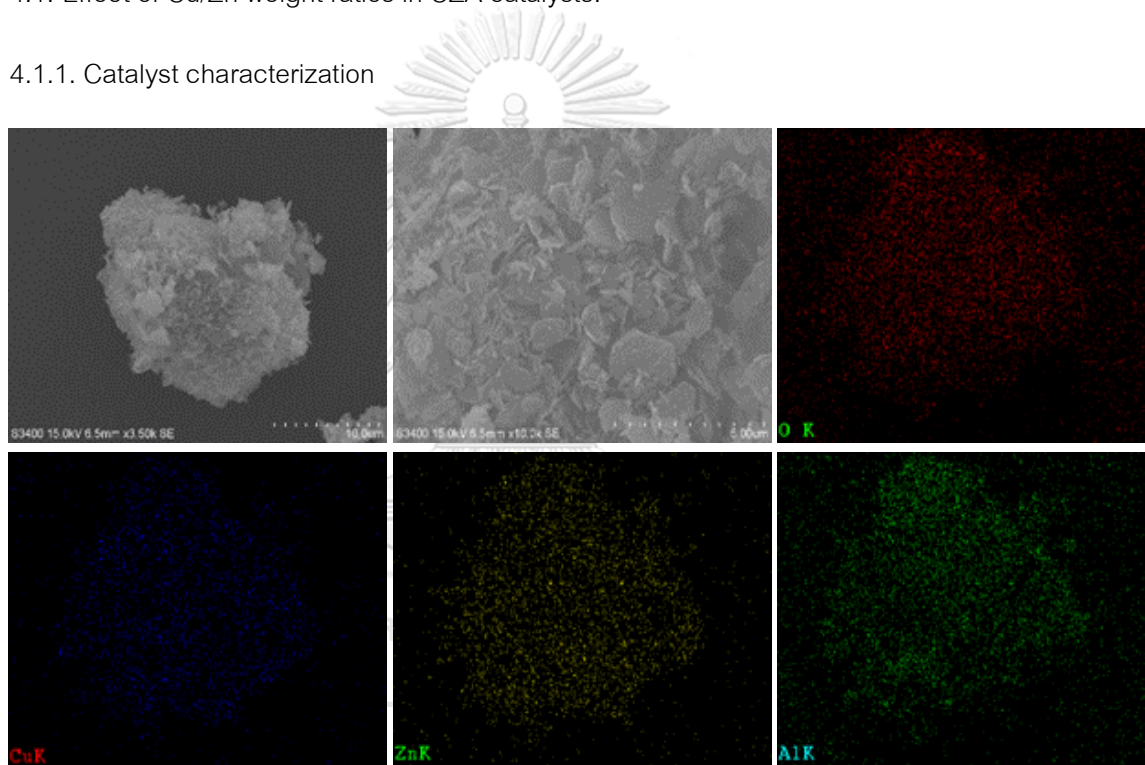


Figure 9. The SEM-EDX images of CZA-0.5 catalyst.

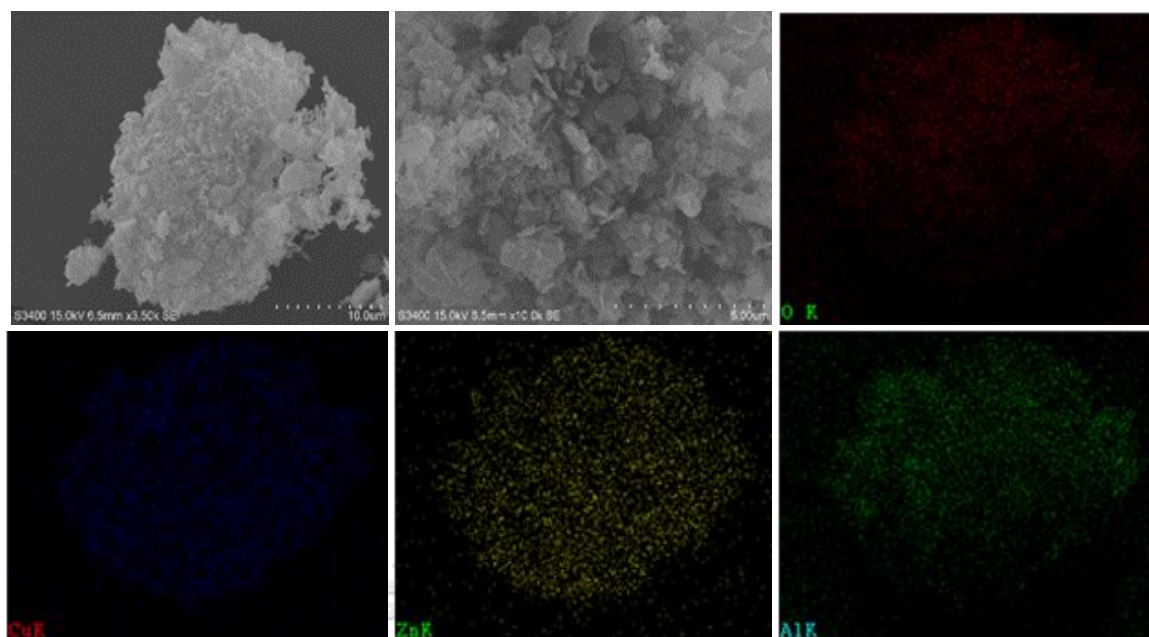


Figure 10. The SEM-EDX images of CZA-1 catalyst.

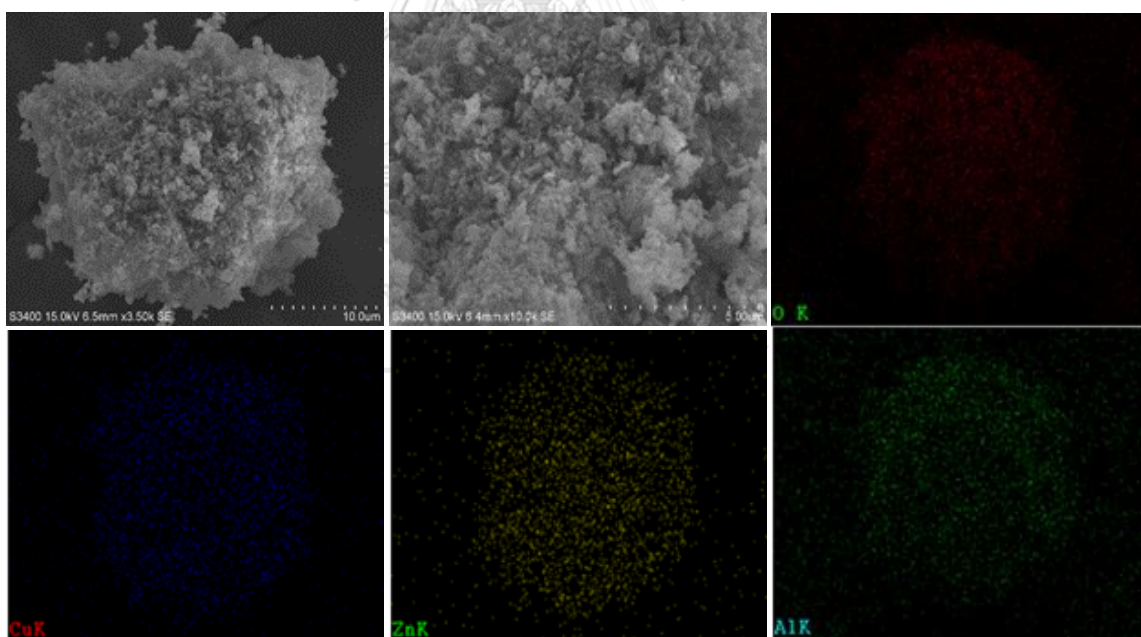


Figure 11. The SEM-EDX images of CZA-2 catalyst.

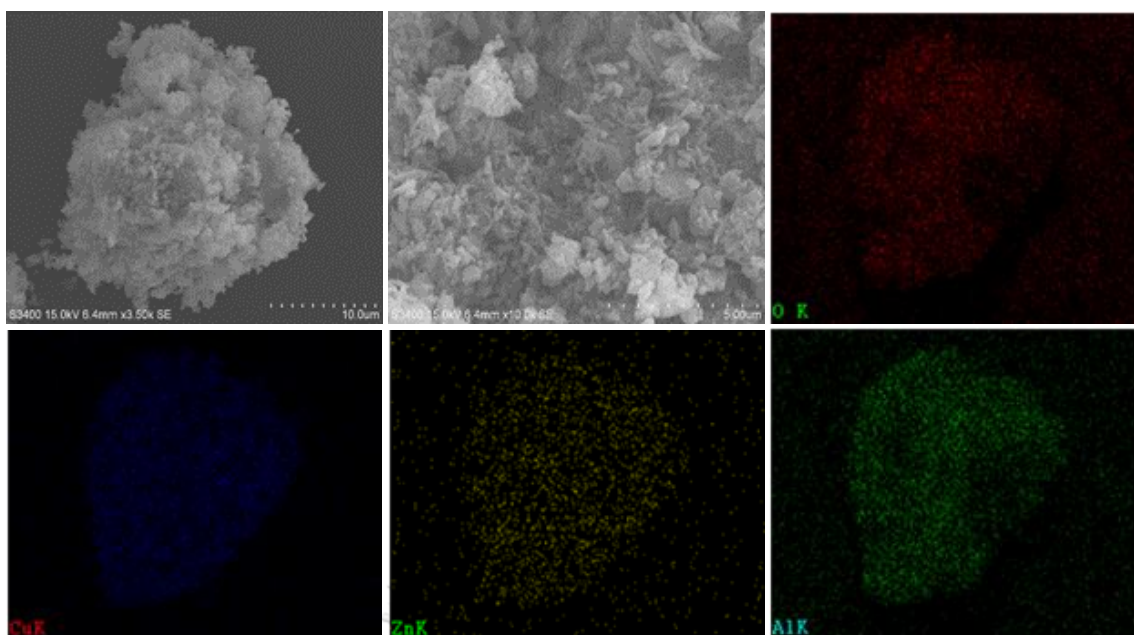


Figure 12. The SEM-EDX images of CZA-3.5 catalyst.

SEM technique was used to determine the different surface morphology of 4 CZA catalysts as shown in Figures 9 to 12. From SEM micrograph, the results presented that the different weight ratios of Cu/Zn do not significantly change the morphology. In order to study elemental distribution and determine amounts of elemental composition near the surface of catalyst, EDX was performed along with SEM. The elemental dispersion from EDX measurement is shown in Figures 9 to 12. It was demonstrated that the dispersion of elements including Cu, Zn and Al for all CZA catalysts are similar with nicely dispersed throughout the catalyst granules. Moreover, elemental composition from EDX measurement (less than 5 microns), which is present in percent weight of all element is listed in Table 10. It was found that the elemental composition of all CZA catalysts obtained from EDX measurement was close to the expected composition of the catalyst.

In addition, ICP-MS technique can be used to determine elemental composition in bulk catalyst. The results obtained from ICP-MS measurement are presented in Table 10. It was observed that the amounts of all elements from ICP-MS measurement was also equal to the amounts of all elements from EDX measurement. Therefore, it apparently indicated the homogeneous elemental distribution throughout the catalyst granules. Moreover, the amounts

of all elements for both EDX and ICP-MS measurement were close to the expected composition of the catalyst.

Table 10. Element distribution of different CZA catalysts.

Element		Cu	Zn	Al	Cu/Zn
CZA-0.5	Expect (wt.%)	30	60	10	0.5
	EDX (wt.%)	24.5	66.8	8.7	0.4
	ICP-MS (wt.%)	24.7	66.1	9.3	0.4
CZA-1	Expect (wt.%)	45	45	10	1
	EDX (wt.%)	39.9	51.6	8.5	0.8
	ICP-MS (wt.%)	39.3	52.7	8.0	0.7
CZA-2	Expect (wt.%)	60	30	10	2
	EDX (wt.%)	57.9	33.7	8.5	1.7
	ICP-MS (wt.%)	56.5	34.9	8.6	1.6
CZA-3.5	Expect (wt.%)	70	20	10	3.5
	EDX (wt.%)	65.7	25.1	9.2	2.6
	ICP-MS (wt.%)	65.8	25.5	8.7	2.6

The XRD patterns of CZA catalysts with different Cu/Zn weight ratios are presented in **Figure 13**, which exhibited the XRD patterns for all CZA catalysts with the absence of alumina diffraction peaks because alumina may present as an amorphous state and/or small quantities of alumina in CAZ catalysts as a result alumina has well dispersion. Another interesting point was observed that the CZA-0.5 catalyst demonstrated only the diffraction peaks of ZnO because of low weight ratio of Cu/Zn. The diffraction peaks of ZnO phase were located at $2\theta = 31.7^\circ, 36.4^\circ, 56.6^\circ, 62.8^\circ$ and 68.0° [26], [41]. When increase weight ratio of Cu/Zn, the diffraction peaks of CuO can be obviously observed. For the CZA-1, CZA-2 and CZA-3.5 catalysts, they exhibited both CuO phase and ZnO phase. However, CZA-2 and CZA-3.5

catalysts showed low intensity peaks of ZnO. The CZA-3.5 catalysts exhibited strong intensity peaks of CuO because of high weight ratio of Cu/Zn. The diffraction peaks of CuO phase were located at $2\theta = 35.5^\circ, 38.8^\circ, 48.5^\circ, 58.1^\circ, 61.6^\circ, 65.9^\circ, 68.3^\circ,$ and 75.2° [35]. The crystallite sizes of CuO nanoparticles in catalyst calculated by Scherrer equation are listed in Table 11. As seen, crystallite sizes of CuO nanoparticles increase with increasing weight ratio of Cu/Zn because high content of copper may accumulate in CZA catalysts. The CuO crystallite size of CZA-3.5 catalyst shows the maximum of 18.8 nm.

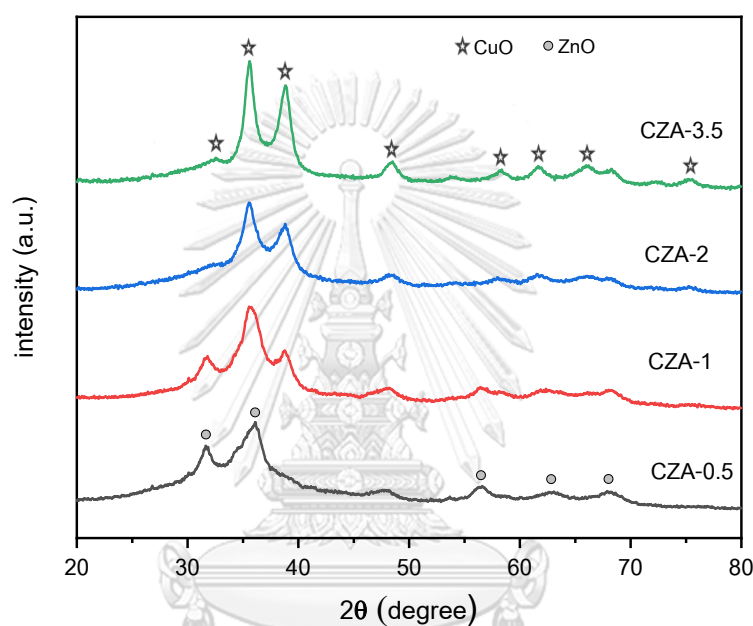


Figure 13. XRD pattern of different CZA catalysts.

Table 11. Textural properties of different CZA catalysts

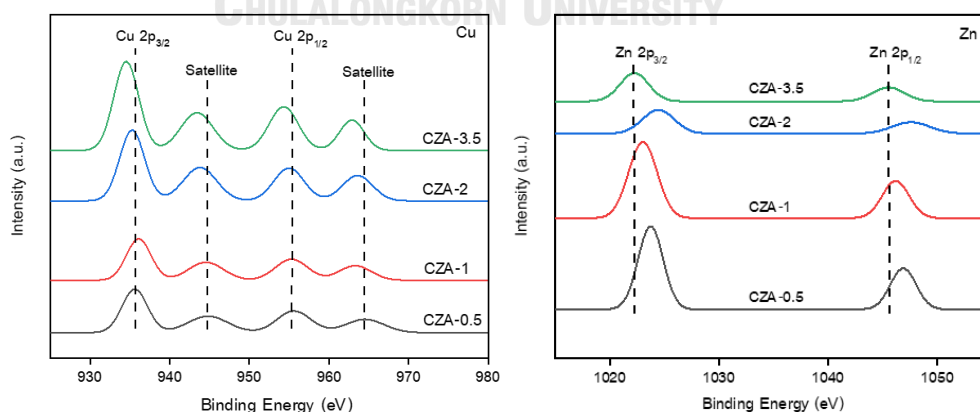
Catalyst	Surface area ^a (m ² /g)	Pore volume ^b (cm ³ /g)	Pore size ^b (nm)	S _{cu} (m ² /g)	D _{cu} (%)	Crystallite size of CuO (nm)
CZA-0.5	36	0.1	12.1	2.6	0.8	6.9
CZA-1	40	0.1	10.1	3.4	1.0	10.7
CZA-2	50	0.2	11.4	8.4	1.3	15.6
CZA-3.5	57	0.2	10.5	10.7	1.4	18.8

^a Determined from BET method

^b Determined from BJH desorption method

N_2 physisorption is a technique which identifies surface area and pore structure of catalysts. Surface area, pore volume and pore size of different CZA catalysts are presented in **Table 11**. The surface area determined from BET method was found to increase with increasing weight ratio of Cu/Zn due to higher Cu content that can result in more generation of porous structure. For pore volume and pore size determined from BJH desorption method, it revealed that the different Cu/Zn weight ratios has little influence on pore volume of CZA catalysts. Pore volume was found to be in range of 0.1-0.2 cm^3/g . Moreover, the different Cu/Zn weight ratios has slightly different of pore size diameter. Pore size of all CZA catalysts was in the range of mesoporous structure (2-50 nm). Pore size was found to be in range of 10.1-12.1 nm.

CO-chemisorption technique was used to measure active metal surface area and dispersion of active sites. The results are shown in **Table 11**. It was observed that the metal surface area is a function of metal loading, in which the metallic copper surface area increases with increase of Cu/Zn weight ratio. Moreover, the results from **Table 11** show that copper dispersion increases with increasing of Cu/Zn weight ratio. Although copper dispersion increased with increasing copper content, it was found that it scarcely increased when Cu/Zn weight ratio is 2. This is attributed to high content of copper causing the agglomeration of copper particle that can be confirmed with XRD results.



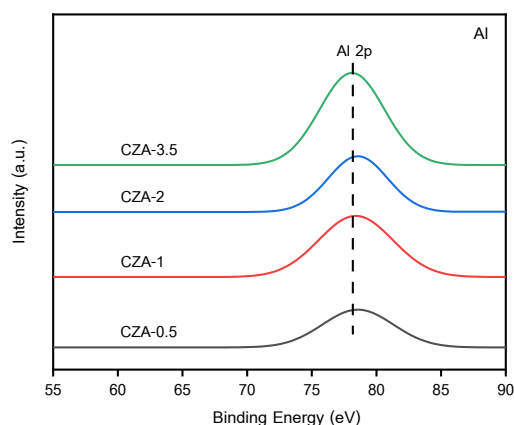


Figure 14. The XPS spectra of all CZA catalysts. (a) The XPS spectra of Cu species, b) The XPS spectra species and c) The XPS spectra of Al species

XPS technique was performed to analyze the surface chemical states of CZA catalysts. The XPS spectra of all CZA catalysts are shown in **Figure 14 (a-c)**. As seen in **Figure 14a**, the XPS spectra presented peaks for Cu $2p_{3/2}$ and Cu $2p_{1/2}$ of all CZA catalysts were located around 934.5-936.2 eV and 954.2-955.5 eV, which is the state of Cu^{2+} for excite state in form Cu^0 ($\text{Cu}^{2+} \rightarrow \text{Cu}^0$). Moreover, there are shakeup satellite peaks around 943.4-944.8 eV and 964.2-968.4 eV that were also identified for Cu^{2+} species. It can be confirmed that only the Cu^{2+} species was present on the CZA catalyst surface. The difference of Cu/Zn weight ratio also affected the amount of Cu^{2+} on catalyst surface, which increases with increasing of Cu/Zn weight ratio. In addition, for CZA-2 and CZA-3.5 catalysts, these peaks show a slight shift to lower binding energy due to charge transfer from ZnO to metal Cu resulting in increasing of electron density on surface Cu species [42]. The binding energy of Zn $2p_{3/2}$ and Zn $2p_{1/2}$ peaks are located around 1022.2-1024.5 eV. and 1045.5-1047.5 eV as seen in **Figure 14b**. It was presented Zn $^{2+}$ species in bulk ZnO. The amount of Zn $^{2+}$ decreases with increasing of Cu/Zn weight ratio. The XPS spectra of Zn 2p for pure ZnO presented peaks at 1021 and 1044.1 eV [43]. For all CZA catalysts, The XPS spectra peaks of Zn show a slight shift to higher binding energy compared to pure ZnO indicating that ZnO acts as the electron donor [43]. At **Figure 14c**, it demonstrates the binding energy of Al 2p peak that was found around 78.5 eV, represented the chemical state of Al^{3+} in Al_2O_3 dispersed on surface of CZA catalysts.

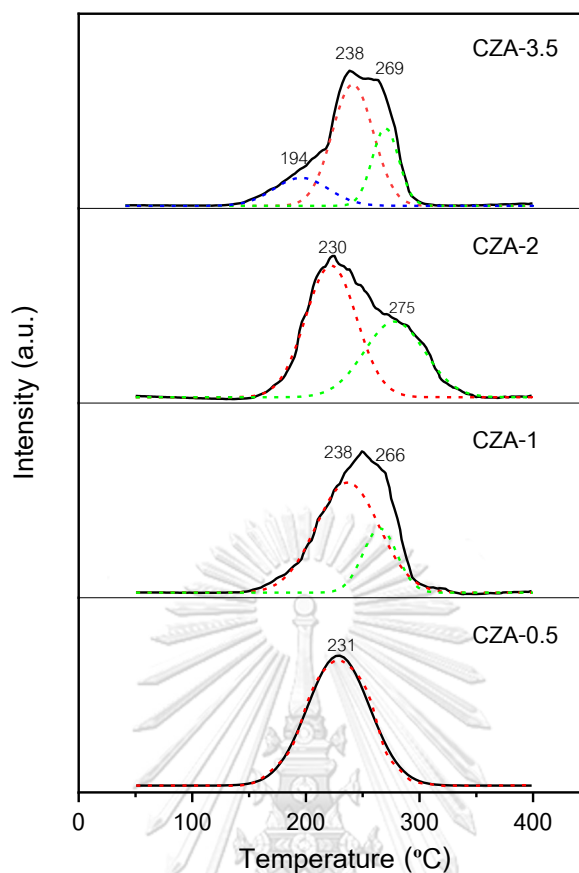


Figure 15. H_2 -TPR profiles of all CZA catalysts.

H_2 -TPR technique was used to analyze the reduction behaviors of CZA catalysts. The TPR profiles of all CZA catalysts are presented in Figure 15. All the CZA catalysts exhibited the reduction below 350 °C. Zn and Al oxide forms cannot be reduced below 350 °C; thus, all the peaks are explained the reduction of CuO phase present in the CZA catalysts. CZA-0.5 catalyst showed only one peak at 231 °C that was ascribed to the surface-dispersed CuO reduction, which include small clusters and isolated copper ions [44]. Another peak was appeared when increasing of Cu/Zn weight ratio, in which peaks were located at 266 °C for CZA-1 catalyst, 275 °C for CZA-2 catalyst and 269 °C for CZA-3.5 catalyst. These peaks were ascribed to the reduction of bulk-like CuO, which include bulk CuO and crystallized copper oxide [44]. For CZA-3.5 catalyst, another peak was appeared at even lower temperatures. It can be ascribed to the reduction in highly dispersed CuO [45]. The reducibility of CZA catalyst decreases with the increasing of Cu/Zn weight ratio due to larger CuO crystallite sizes. These results are in good agreement with those results obtained by XRD analysis.

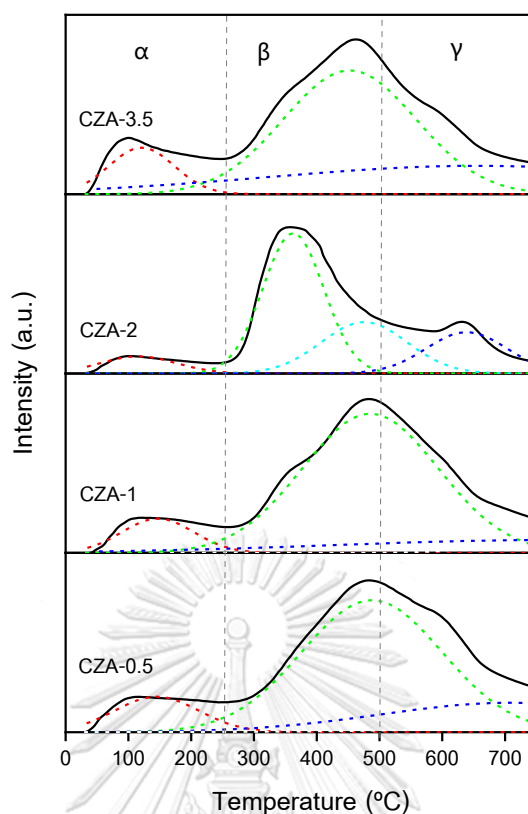


Figure 16. CO₂-TPD profiles of all CZA catalysts.

CO₂-TPD technique was performed to determine the basicity of CZA catalysts. CO₂-TPD profiles of all CZA catalysts are presented in Figure 16. CO₂-TPD profiles can be separated into three regions, which represents three kinds of basic sites. α refers to the weakly basic sites (below 250°C), which is related to the OH groups saturating coordination vacancy (such as alumina). β refers to the moderate basic sites (250-500°C), which assigned to the metal and oxygen pairs. The strong basic sites (above 500°C) were attributed to the coordinatively unsaturated O²⁻ ions [31], which is represented by γ region. The moderate basic site was dominant for all CZA catalysts as seen in Figure 16. In addition, the number of basis sites of all CZA catalysts can be calculated by integration of CO₂ desorption peak area that are summarized in Table 12. It was found that CZA-2 and CZA-3.5 catalyst have the most number of total basic sites, which may result from high specific surface area. Moreover, the number of strongly basic sites increased with increasing of Cu/Zn weight ratio until Cu/Zn is 2, then the number of strongly basic sites dropped to 118.0 $\mu\text{mol/g}_{\text{cat}}$. The number of strongly basic sites of CZA-3.5 catalyst shows the maximum of 230.4 $\mu\text{mol/g}_{\text{cat}}$. The growing strong basic site of CZA-3.5 catalyst due to the metal–oxygen pairs could partially break up [46],

which corresponds to the reduction of moderate basic site. Many researchers proposed that the distribution of strongly basic sites essentially influenced the selectivity of CH₃OH [47].

Table 12. The amounts of basic sites of all CZA catalysts.

Catalyst	Number of basic sites ($\mu\text{mol/g}_{\text{cat}}$)			Number of total basic sites ($\mu\text{mol/g}_{\text{cat}}$)
	Weak	Moderate	Strong	
CZA-0.5	52.8	342.2	140.4	535.4
CZA-1	52.8	326.3	150.4	529.5
CZA-2	42.3	459.3	118.0	619.5
CZA-3.5	58.8	330.3	230.4	619.5

4.1.2 Catalyst performance

The catalytic performance of CZA catalysts was measured in hydrogenation of CO and CO₂ at the reaction temperature of 250 °C under atmospheric pressure. The feed composition of CO/H₂ is 1:2 for CO hydrogenation and CO₂/H₂ is 1:3 for CO₂ hydrogenation. The catalytic activity of CZA catalysts expressed in terms of CO conversion, CO₂ conversion and methanol selectivity, which were followed by time on stream for 5 hours as reported in **Table 13**. The results of the CO hydrogenation over CZA catalysts show that CO conversion increased with increase of Cu/Zn weight ratio showing the similar trend with CO₂ conversion of the CO₂ hydrogenation. This can be explained by the effect of high copper loading causing the high surface area and high copper dispersion. From these results, both CO and CO₂ conversions over CZA catalysts are quite low because of the limit of thermodynamics. Normally, methanol synthesis via hydrogenation of CO and CO₂ is operate under pressure of 30-50 bars resulting in high conversion and this research merely uses atmospheric pressure. However, the results obtained was acceptable when compared to other researches with similar reaction condition [35] [36].

CO hydrogenation over CZA catalysts showed only methanol selectivity as seen in **Table 13**. On the other hand, the CO₂ hydrogenation exhibited scarce methanol selectivity, in which CO is the main product from CO₂ hydrogenation. This is due to CO₂ easily converted to

CO under this condition via the reverse water gas shift (RWGs), which is a side reaction of CO₂ hydrogenation. And this reaction condition (at low pressure) occurs via the monodentate formate intermediate that can easily decompose to CO rather than form to dioxomethylene intermediate for methanol formation [35]. The methanol selectivity of CZA-3.5 catalyst shows the maximum of 0.25%, which is due to the maximum of strongly basic sites. Unidentate carbonates is CO₂ adsorbed species on strongly basic site which is the key intermediate that generates to methanol [28].

Table 13. Catalyst activity of CZA catalysts.

Catalysts	Reaction time 5 h				
	CO hydrogenation		CO ₂ hydrogenation		
	CO conversion (%)	Methanol Selectivity (%)	CO ₂ conversion (%)	CO Selectivity (%)	Methanol Selectivity (%)
CZA-0.5	0.82	100	1.37	99.84	0.16
CZA-1	1.04	100	1.54	99.84	0.16
CZA-2	1.20	100	1.75	99.85	0.15
CZA-3.5	1.27	100	1.87	99.75	0.25

At 250°C under atmospheric pressure.

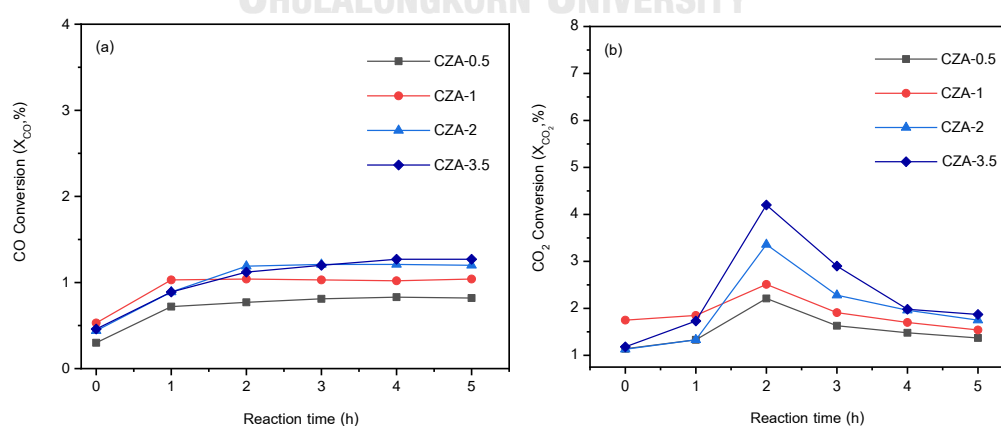


Figure 17. The CO and CO₂ conversion of CZA catalysts in time on stream 5 h. (a) CO hydrogenation (b) CO₂ hydrogenation

From Figure 17, it is shown that the CO conversion of all CZA catalysts increased with increased reaction time until 3 hours, then the CO conversion of all CZA catalysts were quite stable. Meanwhile, the CO₂ conversion of all CZA catalysts increased with increased reaction time until 2 hours, and then the CO₂ conversion of all CZA catalysts started to drop. This result was due to CZA catalysts were deactivated by coke formation on the catalyst surface for CO₂ hydrogenation reaction. The deactivation of CZA catalysts is investigated in third section.

4.2. Effect of ZrO₂ and MnO promoters.

4.2.1. Catalyst characterization

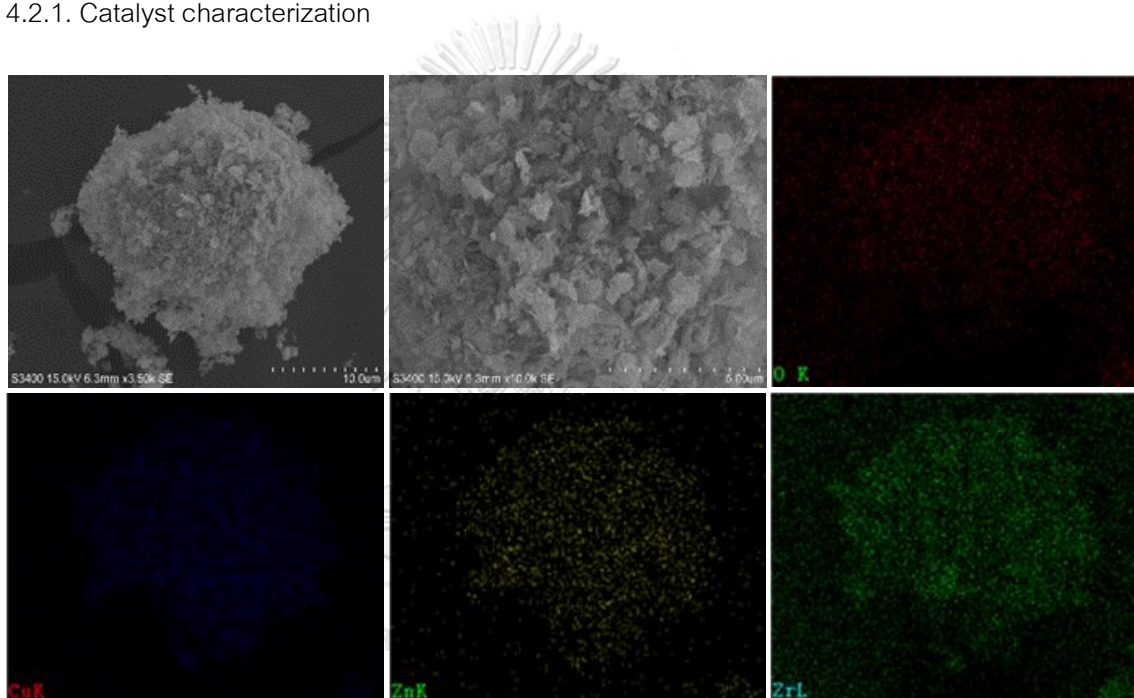
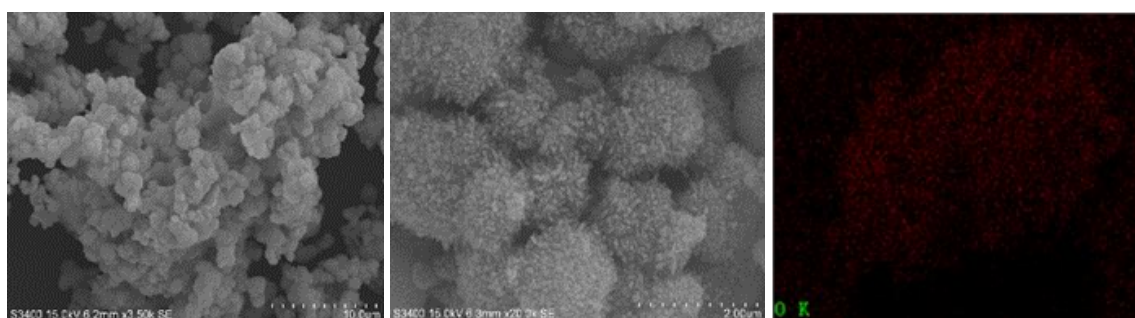


Figure 18. The SEM-EDX images of CZ-Zr-2 catalyst.



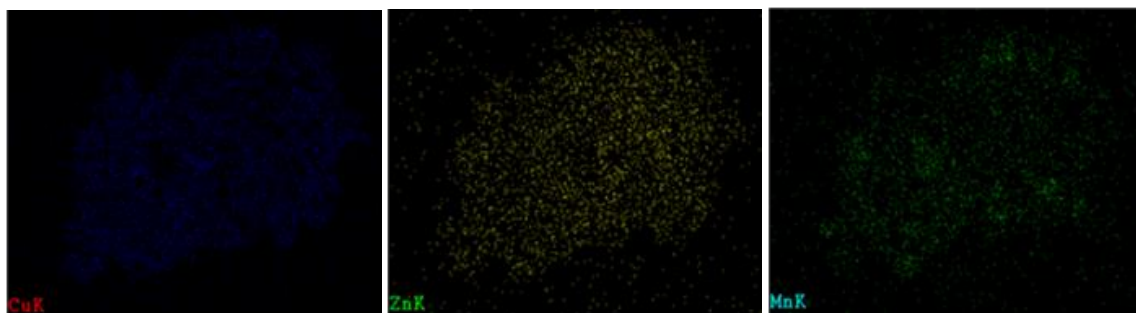


Figure 19. The SEM-EDX images of CZ-Mn-2 catalyst.

SEM micrographs of CZ-Zr-2 and CZ-Mn-2 catalysts are shown in Figures 18 and 19. The results presented the similar morphology of catalysts by comparison of CZA-2 and CZ-Zr-2 catalysts. The morphology of CZ-Mn-2 catalyst was slightly different from other catalysts. The morphology of CZ-Mn-2 catalyst is presented as amorphous shape. The EDX measurement is also presented the elemental distribution of CZ-Zr-2 and CZ-Mn-2 catalysts as seen in Figures 18 and 19, respectively. It was found that both CZ-Zr-2 and CZ-Mn-2 catalysts exhibit similarly well distributed of all element throughout the catalyst granules, which are the same as CZA-2 catalyst. In addition, elemental composition from EDX measurement (less than 5 microns) which presents in percent weight of all element is listed in Table 14. It was found that the elemental composition of both CZ-Zr-2 and CZ-Mn-2 catalysts obtained from EDX analysis was close to the expected composition in the catalyst preparation process.

The elemental composition in bulk catalyst was obtained from ICP-MS analysis is shown in Table 14. It was observed that the amounts of all elements from ICP-MS analysis was equal to the amounts of all elements from EDX analysis. This result can be confirmed the homogeneous elemental dispersion throughout the catalyst granules.

Table 14. Element distribution of CZA-2, CZ-Zr-2 and CZ-Mn-2 catalysts.

Element		Cu	Zn	Al	Zr	Mn	Cu/Zn
CZA-2	Wt% (Expect)	60	30	10	n.a	n.a	2
	EDX (Wt%)	57.9	33.7	8.5	n.a	n.a	1.7
	ICP-MS (Wt%)	56.5	34.9	8.6	n.a	n.a	1.6
CZ-Zr-2	Wt% (Expect)	60	30	n.a	10	n.a	2
	EDX (Wt%)	57.9	32.4	n.a	9.7	n.a	1.8

	ICP-MS (Wt%)	n.d	n.d	n.a	n.d	n.a	n.d
CZ-Mn-2	Wt% (Expect)	60	30	n.a	n.a	10	2
	EDX (Wt%)	57.9	33.5	n.a	n.a	8.7	1.7
	ICP-MS (Wt%)	58.6	32.9	n.a	n.a	8.5	1.8

n.a = not available, n.d = not detected

The XRD patterns of CZA-2, CZ-Zr-2 and CZ-Mn-2 catalysts are shown in **Figure 20**. It was found that CZA-2, CZ-Zr-2 and CZ-Mn-2 catalysts demonstrated both peaks of CuO phase and ZnO phase. In the same way, no diffraction peaks of CZ-Zr-2 and CZ-Mn-2 catalysts were observed for ZrO₂ phase and MnO phase. This is because both Zr and Mn maybe present in small quantities. ZrO₂ and MnO particles are fine and highly dispersed. Nevertheless, Zr species can be promoted to a decreased sharp peak of CuO, but increased peaks of ZnO phase. The dispersion of CuO phase and ZnO phase was promoted by Mn species. The crystallite sizes of CuO nanoparticles are listed in **Table 15**. The promotion of Zr and Mn led to a decrease of CuO crystallite size from 15.6 nm to 9.9 and 13.0 nm, respectively.

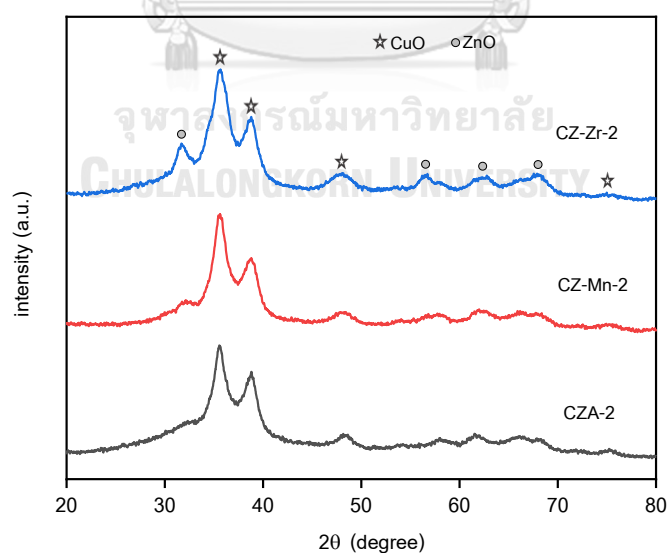


Figure 20. XRD pattern of CZA-2, CZ-Zr-2 and CZ-Mn-2 catalysts.

Table 15. Textural properties of CZA-2, CZ-Zr-2 and CZ-Mn-2 catalysts.

Catalyst	Surface area ^a (m ² /g)	Pore volume ^b (cm ³ /g)	Pore size ^b (nm)	S _{cu} (m ² /g)	D _{cu} (%)	Crystallite size of CuO (nm)
CZA-2	49.5	0.2	11.4	8.4	1.3	15.6
CZ-Zr-2	48.7	0.2	13.2	8.0	1.2	9.9
CZ-Mn-2	84.9	0.3	9.9	10.3	1.6	13.0

^a Determined from BET method

^b Determined from BJH desorption method

The results obtained from N₂ physisorption technique are presented in **Table 15**. The BJH method was applied to determine pore volume and pore size of catalyst. It was found that the different promoter has scarcely influence on pore volume. Pore volume was found to be in range of 0.2-0.3 cm³/g. The pore size of CZ-Zr-2 catalyst is higher than CZA-2 catalyst. Meanwhile, the pore size of CZ-Mn-2 catalyst is smaller than CZA-2 catalyst. The BET method was applied to calculate surface area of catalyst. The surface area of CZ-Zr-2 catalyst was close to the surface area of CZA-2 catalyst. The surface area of CZ-Mn-2 catalyst presents the maximum of 84.9 m²/g and it can be explained that Mn metal can improve surface area of catalyst.

CO-chemisorption technique was used to measure active metal surface area and dispersion of active sites as seen in **Table 15**. The results show that the metallic copper surface area and the copper dispersion of CZ-Zr-2 catalyst were close to the metallic copper surface area and the copper dispersion of CZA-2 catalyst. Meanwhile, Mn metal improves both the metallic copper surface area and the copper dispersion, in which the metallic copper surface area and the copper dispersion of CZ-Mn-2 catalyst are 10.3 and 1.6, respectively.

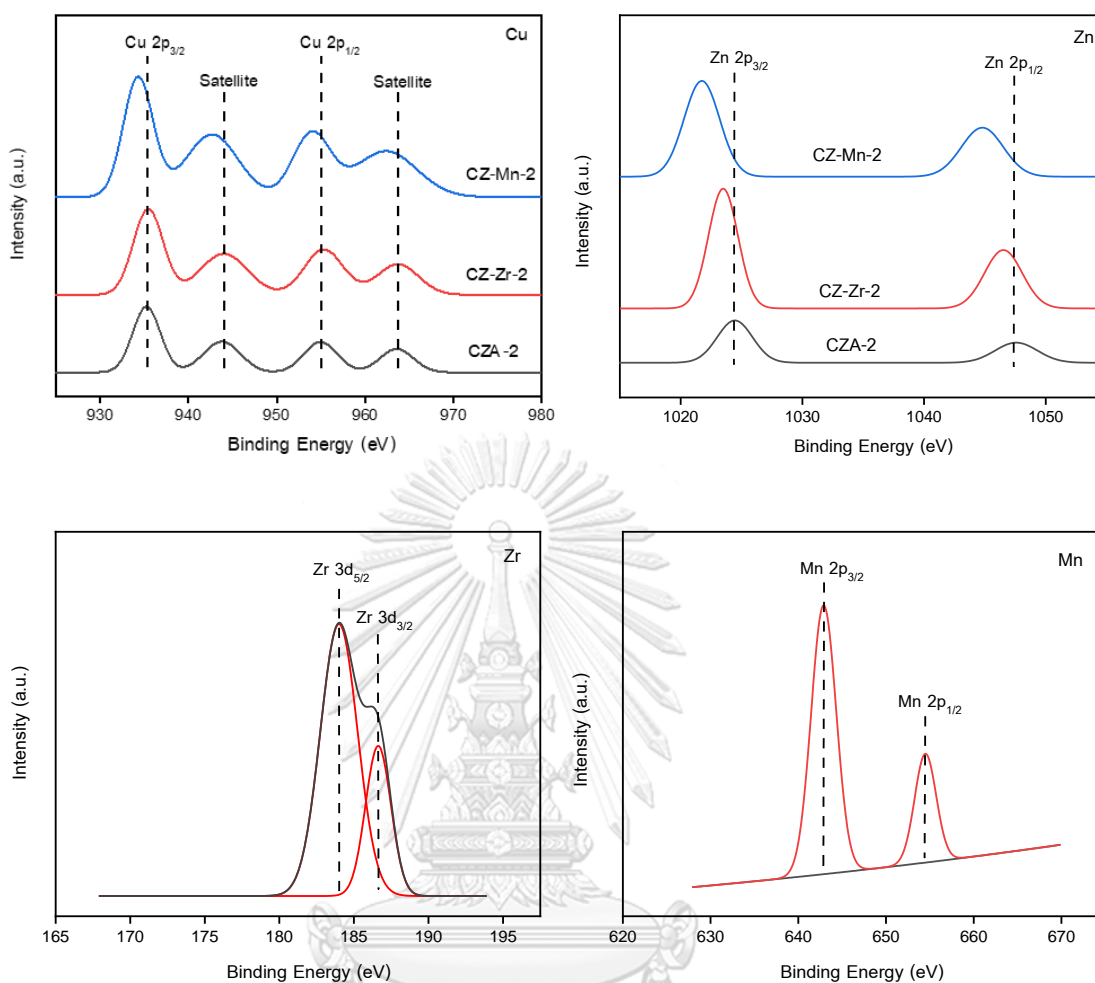


Figure 21. The XPS spectra of CZA-2, CZ-Zr-2 and CZ-Mn-2 catalysts. (a) The XPS spectra of Cu species, b) The XPS spectra of Zn species, c) The XPS spectra of Zr species and d) The XPS spectra of Mn species

The surface chemical states of Cu, Zn, Zr and Mn on the surface catalysts were determined by XPS technique. The XPS spectra of all element are presented in **Figure 21 (a-c)**. In **Figure 21a**, the XPS spectra presented peaks for Cu $2p_{3/2}$ and Cu $2p_{1/2}$ of CZA-2, CZ-Zr-2 and CZ-Mn-2 catalysts that were located around 934.3-935.3 eV. and 954.0-955.1 eV, which is the state of Cu^{2+} species. The other two shakeup satellite peaks around 942.7-944.1 eV. and 962.2-963.7 eV were also identified for Cu^{2+} species. Besides, **Figure 21b** shows Zn $2p_{3/2}$ and Zn $2p_{1/2}$ peaks of CZA-2, CZ-Zr-2 and CZ-Mn-2 catalysts that were located around 1021.7-

1024.5 eV. and 1044.8-1047.5 eV, which were corresponded to Zn^{2+} species in bulk ZnO. The Zr 3d spectra of CZ-Zr-2 catalyst contain two peaks at 184 and 186.5 eV as seen in **Figure 21c**. It was presented Zr $3d_{5/2}$ and Zr $3d_{3/2}$, which is illustrated the existence of Zr^{4+} species on CZ-Zr-2 catalyst surface [48]. **Figure 21d** shows Mn $2p_{3/2}$ and Mn $2p_{1/2}$ peaks of CZ-Mn-2 catalyst that were located at 642.9 and 654.5 eV, respectively. It was presented Mn^{2+} species. As can be seen, MnO led to a shift in the peak of $Zn2p_{3/2}$ and $Zn2p_{1/2}$, which indicated the change in electronic state of Zn^{2+} . In addition, MnO affected to increase the density of active Cu on CZ-Mn-2 catalyst surface [49]. These results are agreeable to CO-chemisorption analysis.

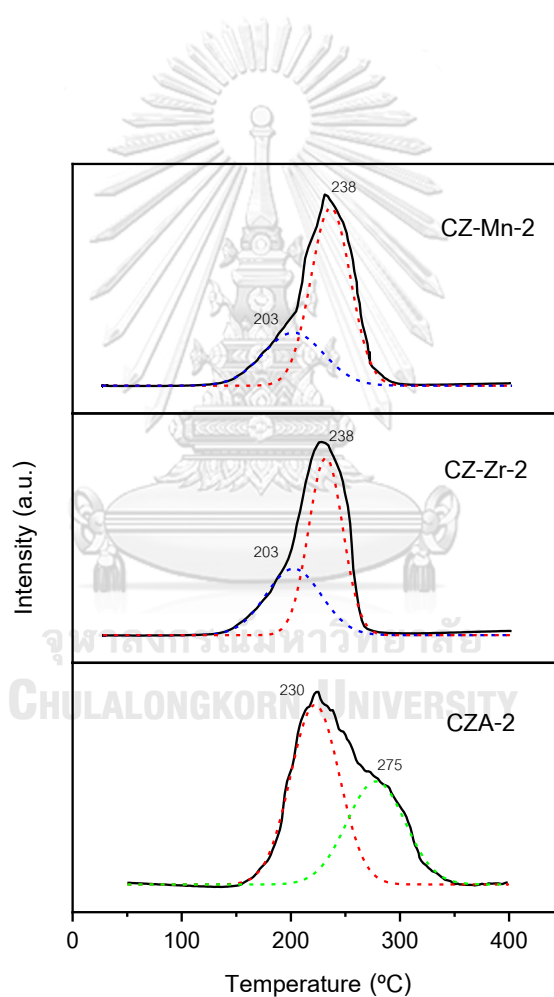


Figure 22. H_2 -TPR profiles of CZA-2, CZ-Zr-2 and CZ-Mn-2 catalysts

The reduction behaviors of CZA-2, CZ-Zr-2 and CZ-Mn-2 catalysts are shown in **Figure 22**, which were obtained from H_2 -TPR analysis. The major reduction peaks of CZA-2,

CZ-Zr-2 and CZ-Mn-2 catalysts are located around 300-338 °C that was ascribed to the surface-dispersed CuO reduction. CZA-2, CZ-Zr-2 and CZ-Mn-2 catalysts exhibit another small shoulder peak. For CZ-Zr-2 and CZ-Mn-2 catalysts, the small shoulder peak shifts to low temperature, which is ascribed to the reduction in highly dispersed CuO. On the other hand, the small shoulder peak of CZA-2 catalyst shifts to high temperature, which is ascribed to the reduction of bulk-like CuO including bulk CuO and crystallized copper oxide. It indicated that the reduction of CZ-Zr-2 and CZ-Mn-2 catalysts is easier than CZA-2 catalyst due to smaller crystallite size of CuO. These results are agreeable to XRD analysis. In addition, the reduction of ZnO, ZrO₂ and MnO did not appear in this experimental condition because it occurred at very high temperature [39].

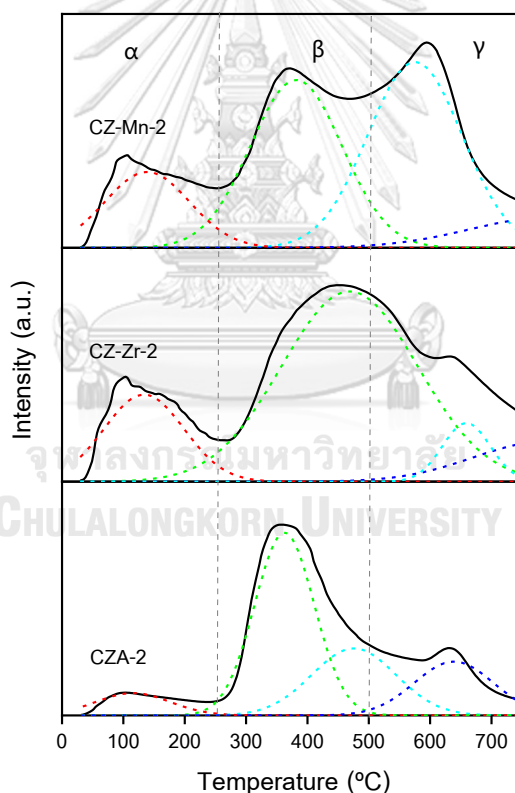


Figure 23. CO₂-TPD profiles of CZA-2, CZ-Zr-2 and CZ-Mn-2 catalysts.

CO₂-TPD profiles of CZA-2, CZ-Zr-2 and CZ-Mn-2 catalysts are presented in Figure 23. CO₂-TPD profiles are separated into three of α , β and γ , which refer to the weak (below 250°C), moderate (250-500°C) and strong (above 500°C) basic sites, respectively. The weak

basic sites are related to the structural OH groups on surface catalysts. The moderate basic sites assigned to interaction between metal and oxygen pairs. The strong basic sites attributed to the coordinatively unsaturated O^{2-} ions [31]. The results show that the moderate basic site was dominant for CZA-2 and CZ-Zr-2 catalysts. Meanwhile, the CZ-Mn-2 catalyst presented the moderate basic sites and the strong basic sites as equally. In addition, the number of basic sites of CZA-2, CZ-Zr-2 and CZ-Mn-2 catalysts can be calculated by integration of CO_2 desorption peak area, that are summarized in **Table 16**. CZA-2, CZ-Zr-2 and CZ-Mn-2 catalysts have the same amounts of total basic sites. The number of strong basic sites increase in the series $CZA-2 < CZ-Zr-2 < CZ-Mn-2$. CZ-Mn-2 catalyst exhibits the highest amounts of strong basic sites that was $277.2 \mu\text{mol/g}_{\text{cat}}$. On the other hand, the number of moderate basic sites decrease for CZ-Zr-2 and CZ-Mn-2 catalysts. These results occur because the metal–oxygen pairs could partially break up, which procreated to unsaturated O^{2-} ions. Zr and Mn metals led to an increase in the number of strong basic sites.

Table 16. The amounts of basic sites of CZA-2, CZ-Zr-2 and CZ-Mn-2 catalysts.

Catalyst	Number of basic sites ($\mu\text{mol/g}_{\text{cat}}$)			Number of total basic sites ($\mu\text{mol/g}_{\text{cat}}$)
	Weak	Moderate	Strong	
CZA-2	42.3	459.3	118.0	619.5
CZ-Zr-2	97.0	368.9	153.7	619.5
CZ-Mn-2	89.8	252.6	277.2	619.5

4.2.2 Catalyst performance

In second part, the CZ-Zr-2 and CZ-Mn-2 catalysts were measured in CO hydrogenation and CO_2 hydrogenation compared with the CZA-2 catalyst from the previous part. The effect of Zr and Mn promoters to CO hydrogenation and CO_2 hydrogenation is observed in **Table 17**. The result showed that the CZ-Zr-2 and CZ-Mn-2 catalysts exhibited higher conversion of CO than CZA-2 catalyst due to the increase of weak basic sites. OH group is surface function on weak basic sites when CO adsorbed on weak basic sites, it can

generate to formate intermediate (HCOO). The formate intermediate is the key intermediate of methanol synthesis. Meanwhile, amount of weak basic sites on CZ-Mn-2 catalyst was close to CZ-Zr-2 catalyst but CO conversion of CZ-Mn-2 catalyst was lower than CZ-Zr-2 catalyst because the strong adsorption of CO on CZ-Mn-2 catalyst is difficultly desorbed. The highest CO conversion is obtained on the CZ-Zr-2 catalyst (ca.1.57%). CO hydrogenation over CZA-2, CZ-Zr-2 and CZ-Mn-2 catalysts showed only methanol selectivity. For CO₂ hydrogenation, the maximum CO₂ conversion was obtained over CZ-Mn-2 catalyst (ca.5.63%), which is high when compared with equilibrium conversion [50]. On the other hand, the Zr promoter led to the decrease of CO₂ conversion. The methanol selectivity for CO₂ hydrogenation increases in the series CZA-2 < CZ-Zr-2 < CZ-Mn-2. The methanol selectivity of CZ-Mn-2 catalyst shows the maximum of 0.21%, which is due to the maximum of strong basic sites.

Table 17. Catalyst activity of CZA-2, CZ-Zr-2 and CZ-Mn-2 catalysts.

Catalysts	Reaction time 5 h				
	CO hydrogenation		CO ₂ hydrogenation		
	CO conversion (%)	Methanol Selectivity (%)	CO ₂ conversion (%)	CO Selectivity (%)	Methanol Selectivity (%)
CZA-2	1.20	100	1.75	99.85	0.15
CZ-Zr-2	1.57	100	1.50	99.84	0.16
CZ-Mn-2	1.21	100	5.63	99.79	0.21

At 250°C under atmospheric pressure.

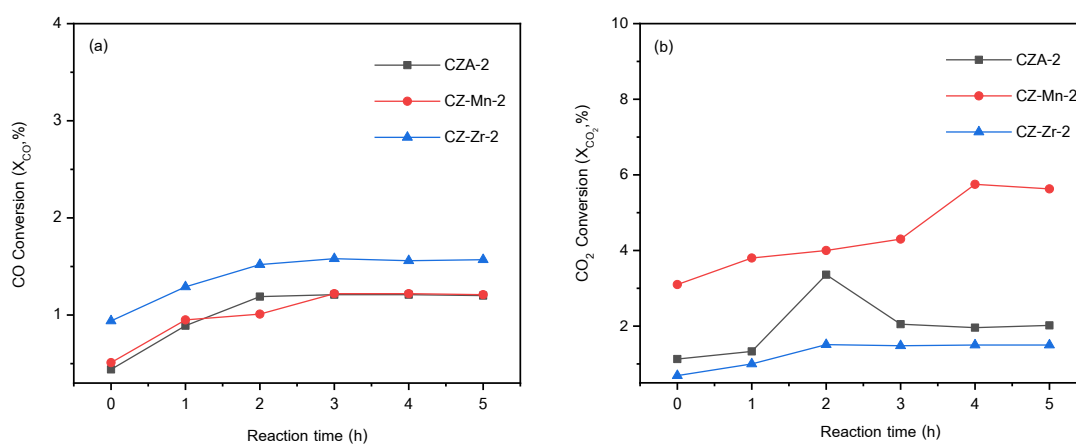


Figure 24. The CO and CO₂ conversion of CZA catalysts in time on stream 5 h. (a) CO hydrogenation (b) CO₂ hydrogenation

Figure 24 presents the CO conversion of CZA-2, CZ-Zr-2 and CZ-Mn-2 catalysts which increased with increasing reaction time until 3 hours, then they were quite stable. For CO₂ hydrogenation, Zr and Mn promoters led to enhancement of CZA catalyst deactivation as shown in **Figure 24b**. The CO₂ conversion of CZ-Zr-2 catalyst increased with increasing reaction time until 2 hours, after that it was stable. Similarly, the CO₂ conversion of CZ-Mn-2 catalyst increased with increasing reaction time until 4 hours, then they were quite stable.

4.3. The deactivation of catalysts

The section investigates the reason of catalyst deactivation for CO₂ hydrogenation. There are several reasons that led to catalyst deactivation, such as chemical poisoning, fouling, coking and sintering. However, the chemical poisoning seems to be impossible because the reactants that were used in our methanol synthesis are pure substance (UHP grade). Therefore, it is assumed that the catalyst deactivation may arise from coking or sintering on the catalyst surface.

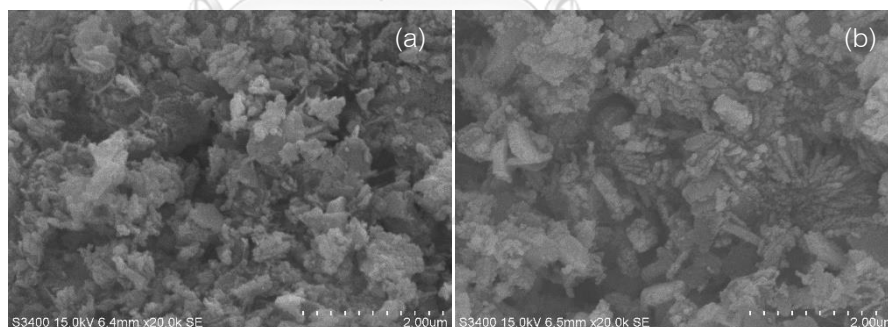


Figure 25. SEM images of fresh CZA-2 catalyst (a), spent sCZA-2 catalyst (b)

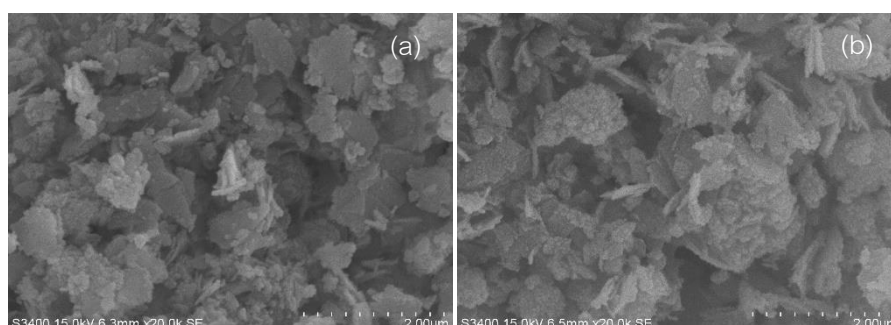


Figure 26. SEM images of fresh CZ-Zr-2 catalyst (a), spent sCZ-Zr-2 catalyst (b)

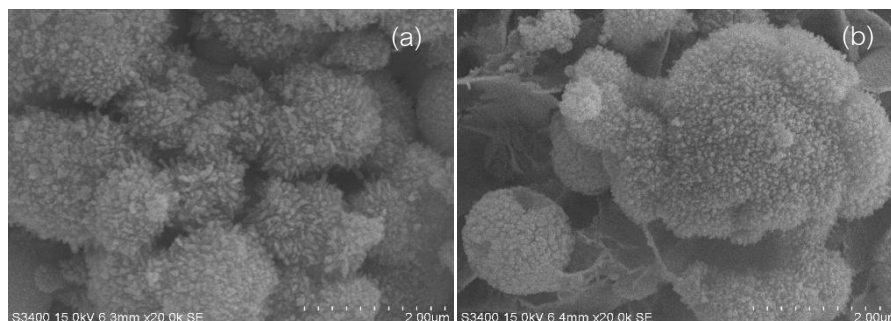


Figure 27. SEM images of fresh CZ-Mn-2 catalyst (a), spent sCZ-Mn-2 catalyst (b)

SEM technique was used to determine the different surface morphology of catalyst. SEM images of fresh catalyst compared with spent catalyst are shown in Figure 25-27. After tested in CO₂ hydrogenation for 5 hours, the morphologies of spent catalysts do not significantly change from the morphology fresh catalysts.

EDX technique was used to determine elemental distribution on spent catalysts, which presented in percent weight of each element as shown in Table 18. It can be found that elemental weight ratio of catalysts after reaction test is about 60:30:10. The results are similar as fresh catalysts. Moreover, carbon was slightly occurred on surface of spent catalyst. The amounts of carbon increases in the series of CZ-Mn-2 < CZ-Zr-2 < CZA-2. Carbon contents presented in CZ-Mn-2 catalyst may refer to carbon in precursor of carbonated compound because it was very poor carbon contents. For CZA-2 and CZ-Zr-2 catalysts, carbon contents may refer to the coke formation after CO₂ hydrogenation.

Table 18. EDX elemental analysis on spent catalysts

Element	Cu	Zn	Al	Zr	Mn	C
sCZA-2	60.50	27.89	8.28	n.a	n.a	3.33
sCZ-Zr-2	59.47	29.66	n.a	9.55	n.a	1.32
sCZ-Mn-2	58.69	30.16	n.a	n.a	10.22	0.93

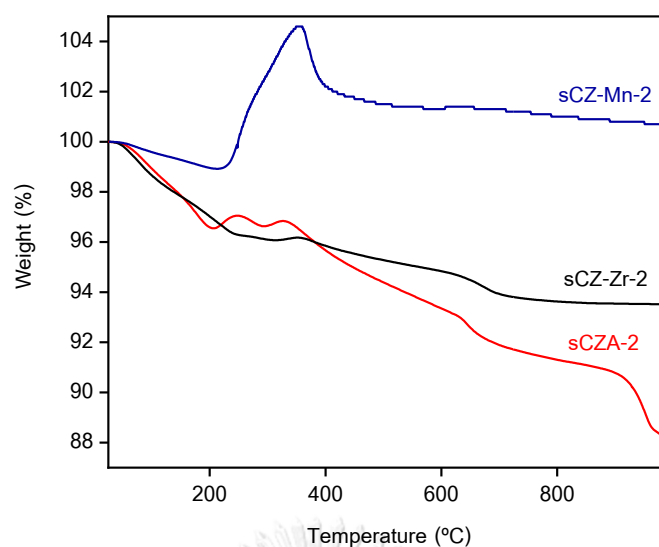


Figure 28. TG profile of spent catalysts (after CO₂ hydrogenation for 5 h)

The thermogravimetric analysis (TGA) was used to investigate the presence of coke in the form of carbon on the spent catalyst surface as shown in Figure 28. At first stage (below 220 °C), CZA-2, CZ-Zr-2 and CZ-Mn-2 catalysts demonstrated similar behavior. It can be assigned to adsorbed water in the spent catalysts. The CZ-Mn-2 catalyst exhibited increase of weight after 220 °C, which is probably caused by copper oxidation from C⁰ that remained in catalyst after reaction test. The weight losses of spent CZA-2 and CZ-Zr-2 catalysts in the temperature range of 330-690 °C were due to coke combustion losses. The weight losses due to the carbon deposited in the temperature range 330–690 °C of spent CZA-2 and CZ-Zr2 catalysts were 4.56 % and 2.10%, respectively. The carbon deposition in these temperature range can be classified in amorphous carbon [51]. In addition, the CZA-2 catalyst shows another type of weight loss in temperature range of 900-1000 °C, corresponding to a graphitic coke deposited on catalyst support [52], which was the primary reason for the CZA catalyst deactivation in the first section.

CHAPTER 5

CONCLUSIONS AND RECOMMENDATIONS

In this research, the effects of Cu/Zn ratios and Mn or Zr promoters on characteristics, activity and stability of CuO/ZnO-based catalysts were examined via hydrogenation of CO and CO₂. Consequently, the results were summarized into 3 parts as follows;

Part 1: The effect of Cu/Zn weight ratios in CZA catalysts

The surface area, metallic copper surface, copper dispersion and number of total basic sites increased with increasing of Cu/Zn weight ratio. These results led to increasing catalytic activity for both methanol synthesis via CO and CO₂ hydrogenation. Therefore, the CZA-3.5 catalyst exhibited the highest catalytic activity having 1.27% CO conversion, 1.87% CO₂ conversion, 100% methanol selectivity for CO hydrogenation and 0.25% methanol selectivity for CO₂ hydrogenation. Moreover, the minimum number of strong basic sites for CZA-2 catalyst induced the lowest methanol selectivity in CO₂ hydrogenation reaction. The major product obtained from CZA catalysts via CO₂ hydrogenation was CO because the reaction was carried out at low pressure. In addition, CZA catalysts deactivated after 2 hours for CO₂ hydrogenation reaction.

Part 2: The effect of Zr and Mn promoters on CuO/ZnO-based catalyst

Both Zr and Mn can decrease the crystallite size of CuO leading to increasing reducibility. The CZ-Mn-2 catalyst has the highest catalytic activity for CO₂ hydrogenation with 5.63% CO₂ conversion and 0.21% methanol selectivity due to higher the surface area, metallic copper surface, copper dispersion and number of strong basic sites. For CO hydrogenation, the catalytic activity of CZ-Zr-2 catalyst shows the maximum at 1.57% CO conversion, 100% methanol selectivity due to the highest amount of weak basic sites. Additionally, the Zr and Mn promoters can improve the stability of catalyst.

Part 3: The deactivation of catalysts

The carbon deposition on catalyst increases in the series of CZ-Mn-2 < CZ-Zr-2 < CZA-2. The spent CZA-2 catalyst was found to contain both amorphous coke and graphitic coke. For CZ-Zr-2 and CZ-Mn-2 catalysts, they were found to have only amorphous coke.

However, carbon deposition on CZ-Zr-2 and CZ-Mn-2 catalysts was present only small quantities.

Recommendations

1. The metallic copper surface area is recommended to measure by the decomposition of N_2O better than CO-chemisorption technique.
2. The effect of CZA, CZ-Zr and CZ-Mn catalysts to methanol synthesis via hydrogenation of mixed CO and CO_2 was interested.
3. In this research, the reaction was operated at low pressure leading to low CO conversion, CO_2 conversion and methanol selectivity for CO_2 hydrogenation. Therefore, the reaction must be operated at higher pressure for higher catalytic activity.
4. To study stability of CZA, CZ-Zr and CZ-Mn catalysts for CO hydrogenation reaction, it should increase time of reaction to be longer.
5. To study catalyst deactivation, other techniques should be used to characterize the spent catalyst, for comprehend intrinsic cause of catalyst deactivation. For example, XPS was used to investigate the chemical state of spent catalyst.

APPENDIX

APPENDIX.A CALCULATION OF CATALYST PERFORMANCE

A.1 CO conversion

$$\text{CO conversion (\%)} = \frac{\text{CO}_{\text{in}} - \text{CO}_{\text{out}}}{\text{CO}_{\text{in}}} \times 100$$

A.2 CO₂ conversion

$$\text{CO}_2 \text{ conversion (\%)} = \frac{\text{CO}_{2,\text{in}} - \text{CO}_{2,\text{out}}}{\text{CO}_{2,\text{in}}} \times 100$$

A.3 Methanol selectivity

$$\text{CH}_3\text{OH selectivity (\%)} = \frac{\text{mole of Methanol}}{\text{All products}} \times 100$$

A.4 Carbon monoxide selectivity

$$\text{CO selectivity (\%)} = \text{All products} - \text{mole of Methanol}$$

A.5 Methanol yield

$$\text{CH}_3\text{OH yield (\%)} = \frac{\text{CH}_3\text{OH selectivity (\%)} \times \text{Conversion (\%)}}{100}$$

Table A.5.1 Methanol yield on catalysts of CO hydrogenation.

Time (h)	Methanol yield (%)					
	CZA-0.5	CZA-1	CZA-2	CZA-3.5	CZ-Zr-2	CZ-Mn-2
0	0.302	0.531	0.440	0.458	0.511	0.942
1	0.717	1.031	0.891	0.892	0.945	1.294
2	0.768	1.039	1.189	1.122	1.007	1.522
3	0.808	1.026	1.207	1.199	1.216	1.576
4	0.832	1.016	1.212	1.266	1.224	1.558
5	0.823	1.038	1.198	1.272	1.206	1.572

Table A.5.2 Methanol yield on catalysts of CO₂ hydrogenation.

Time (h)	Methanol yield (%)					
	CZA-0.5	CZA-1	CZA-2	CZA-3.5	CZ-Zr-2	CZ-Mn-2
0	0.002	0.003	0.002	0.003	0.001	0.006
1	0.002	0.003	0.002	0.004	0.002	0.008
2	0.004	0.004	0.005	0.011	0.002	0.008
3	0.003	0.003	0.004	0.007	0.003	0.009
4	0.002	0.003	0.003	0.005	0.002	0.012
5	0.002	0.003	0.003	0.005	0.002	0.012



APPENDIX.B CALCULATION OF CRYSTALLITE SIZE

B1. The Scherrer equation

$$D = \frac{K\lambda}{\beta \cos\theta}$$

Where D = Volume average crystallite size, (\AA)

K = unity constant factor, (0.9)

λ = X-ray wavelength, $\text{CuK}\alpha$ radiation, ($\lambda = 1.5406 \text{ \AA}$)

θ = the position of observe peak (degree)

β = X-ray diffraction broadening in half peak, (radian).



APPENDIX.C CALBRATION

C.1 CO calibration

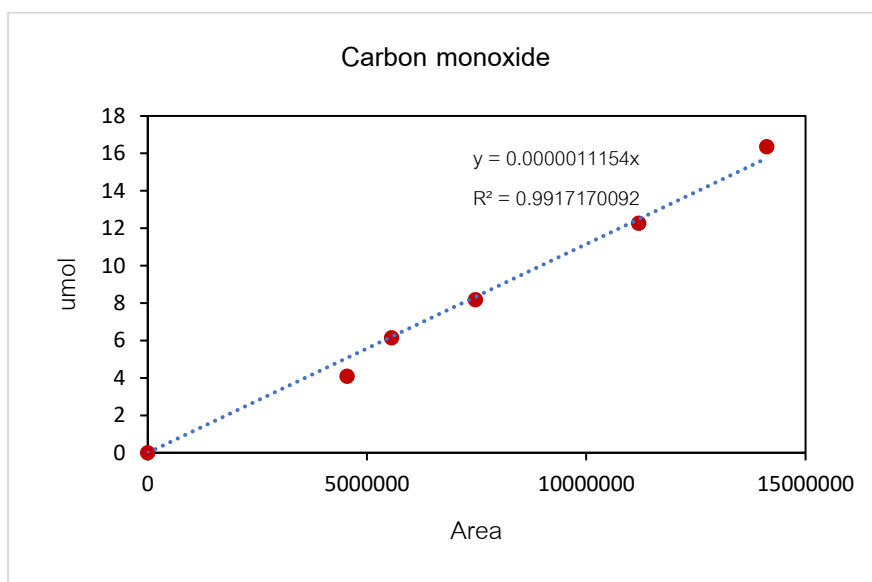
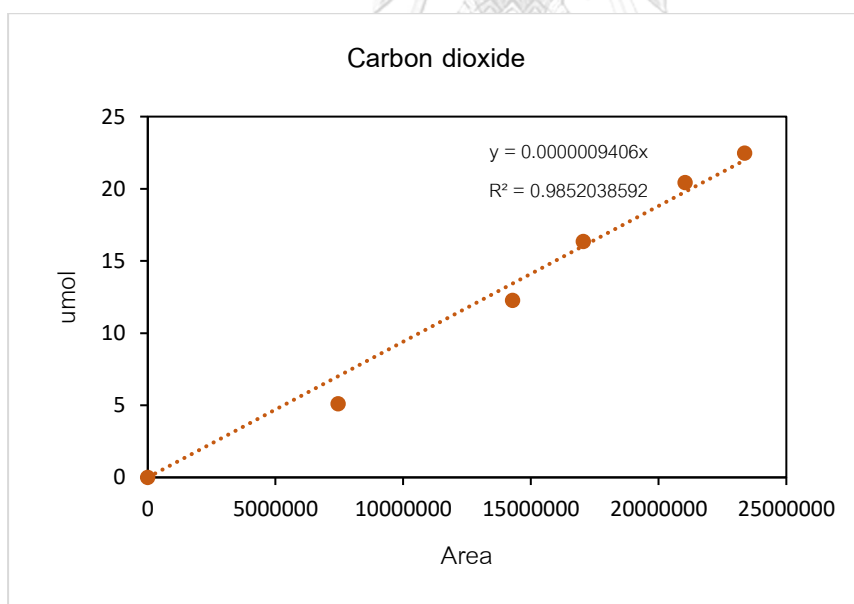


Figure C.1.1 The calibration of CO.

C.2 CO₂ calibrationFigure C.2.1 The calibration of CO₂.

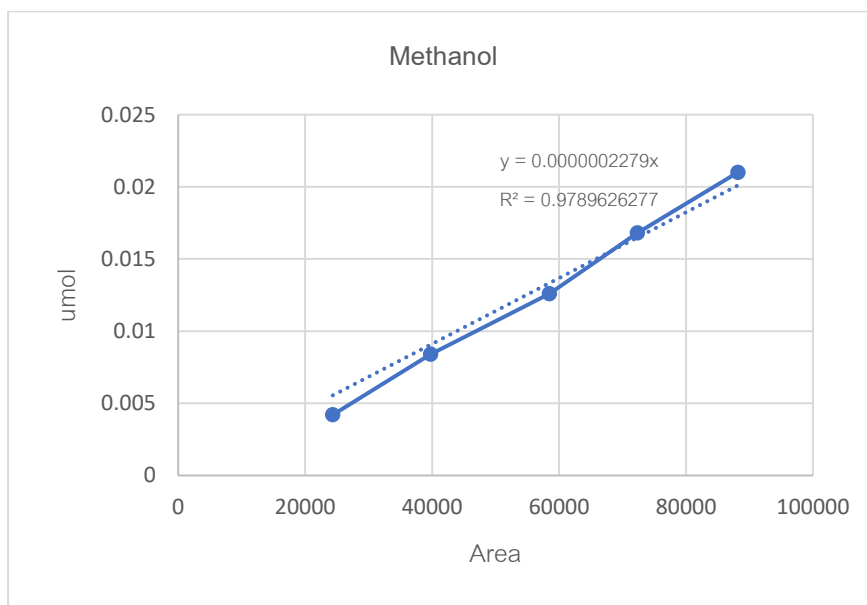
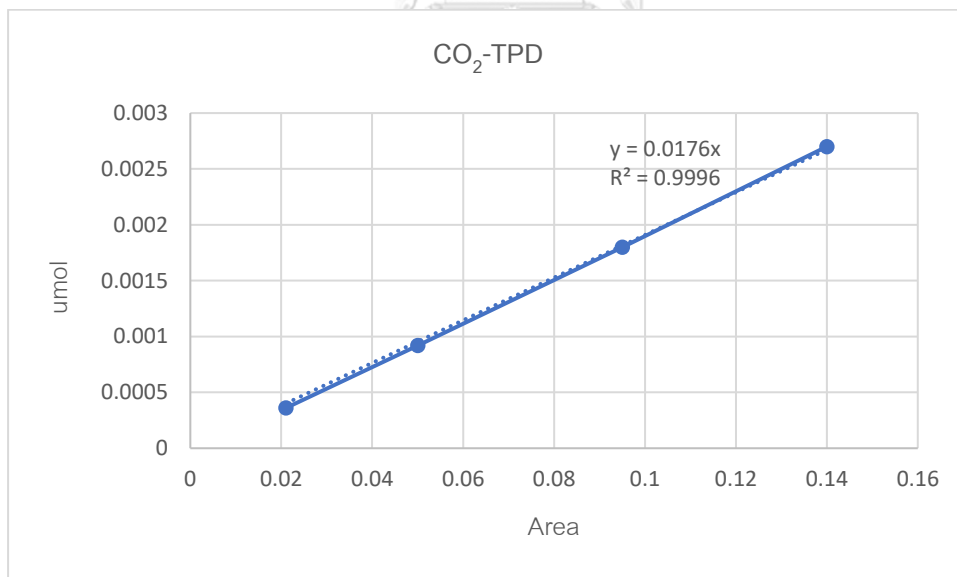
C.3 CH₃OH calibration

Figure C.3.1 The calibration of methanol.

C.4 CO₂-TPD calibrationFigure C.4.1 The calibration of CO₂-TPD.

APPENDIX.D CO-CHEMISORPTION

D.1 Calculation the number of surface-active sites

$$MSA_S = S_f \times \frac{V_{ads}}{V_g} \times \frac{100\%}{\%M} \times N_A \times \sigma_m \times \frac{m^2}{10^{18}nm^2}$$

Where MSA_S = surface-active sites

S_f = stoichiometry factor

V_{ads} = volume adsorbed, (cm³/g)

V_g = molar volume of gas at STP, 22414 (cm³/mol)

N_A = Avogadro's number, 6.023x10²³ (molecules/mol)

σ_m = cross-sectional area of active metal atom, (nm²)

D.2 Calculation active sites dispersion

$$D (\%) = S_f \times \frac{V_{ads}}{V_g} \times \frac{m. w.}{\%M} \times 100\%100\%$$

Where S_f = stoichiometry factor

V_{ads} = volume adsorbed, (cm³/g)

V_g = molar volume of gas at STP, 22414 (cm³/mol)

m. w. = molecular weight of the metal, (a.m.u.)

$\%M$ = % metal, (%)

D.3 Calculation volume chemisorbed in CO-Chemisorption

$$V_{ads}(cm^3) = \frac{V_{inj}}{m} \times \sum_{i=1}^n \left(1 - \frac{A_i}{A_f}\right)$$

Where V_{inj} = volume injected, cm³

m = mass of sample, g

A_i = area of peak i

A_f = area of last peak

Table D.3.1 Area of each peak of CZA-0.5 catalyst adsorbed CO gas.

Peak Number	Area
1	0.09613
2	0.13878
3	0.15118
4	0.15157
5	0.15259
6	0.15760
7	0.15941

Table D.3.2 Area of each peak of CZA-1 catalyst adsorbed CO gas.

Peak Number	Area
1	0.18082
2	0.18700
3	0.20580
4	0.20543
5	0.19993
6	0.21930

Table D.3.3 Area of each peak of CZA-2 catalyst adsorbed CO gas.

Peak Number	Area
1	0.14143
2	0.15072
3	0.17008
4	0.20035
5	0.19077
6	0.21906
7	0.21045

Table D.3.4 Area of each peak of CZA-3.5 catalyst adsorbed CO gas.

Peak Number	Area
1	0.17513
2	0.14147
3	0.13562
4	0.15268
5	0.18384
6	0.19633
7	0.20712
8	0.21302

Table D.3.5 Area of each peak of CZ-Zr-2 catalyst adsorbed CO gas.

Peak Number	Area
1	0.14540
2	0.15061
3	0.15041
4	0.17015
5	0.17034
6	0.19930
7	0.19532
8	0.19732

Table D.3.6 Area of each peak of CZ-Mn-2 catalyst adsorbed CO gas.

Peak Number	Area
1	0.10230
2	0.12354
3	0.14994
4	0.14813
5	0.16158
6	0.16148
7	0.19649
8	0.19513

APPENDIX.E CALCULATION OF BASICITY

E.1 Calculation the number of basic sites

$$\text{number of basic sites } (\mu\text{mole}) = \frac{17.6 \times A}{W}$$

Where A = area under curve of CO_2 -TPD profile of the catalyst sample (area)

W = weight of catalyst sample (g)



REFERENCES

1. Demirel, Y., *Energy: Production, Conversion, Storage, Conservation, and Coupling*. Springer-Verlag London Limited; .
2. Dincer, I. and C. Acar, *Review and evaluation of hydrogen production methods for better sustainability*. *International Journal of Hydrogen Energy*, 2015. **40**.
3. Lachowska, M. and J. Skrzypek, *Methanol synthesis from carbon dioxide and hydrogen over Mn-promoted copper/zinc/zirconia catalysts*. *Reaction Kinetics and Catalysis Letters*, 2004. **83**(2): p. 269-273.
4. Arena, F., et al., *Synthesis, characterization and activity pattern of Cu–ZnO/ZrO₂ catalysts in the hydrogenation of carbon dioxide to methanol*. *Journal of Catalysis*, 2007. **249**(2): p. 185-194.
5. Merck KGaA, D., Germany, 2020; Available from: <https://www.sigmaaldrich.com/chemistry/solvents/methanol-center.html>.
6. National Center for Biotechnology Information, R.P., USA, Methanol; Available from: <https://pubchem.ncbi.nlm.nih.gov/compound/Methanol#section=FIFRA-Requirements>.
7. Schumann, J., *Cu, Zn-based catalysts for methanol synthesis*, in *Technische Universität Berlin, Fakultät II - Mathematik und Naturwissenschaften*. 2015, Technische Universität Berlin: Berlin.
8. Gogate, M.R., *Methanol synthesis revisited: reaction mechanisms in CO/CO₂ hydrogenation over Cu/ZnO and DFT analysis*. *Petroleum Science and Technology*, 2019. **37**(5): p. 603-610.
9. Semelsberger, T.A., et al., *Generating hydrogen-rich fuel-cell feeds from dimethyl ether (DME) using physical mixtures of a commercial Cu/Zn/Al₂O₃ catalyst and several solid–acid catalysts*. *Applied Catalysis B: Environmental*, 2006. **65**(3): p. 291-300.
10. Young, A., et al., *Short Review: Mitigation of Current Environmental Concerns from Methanol Synthesis*. *Bulletin of Chemical Reaction Engineering & Catalysis*, 2013.

- 8.
11. Reubroycharoen, P., et al., *Development of a new low-temperature methanol synthesis process*. Catalysis Today - CATAL TODAY, 2004. **89**: p. 447-454.
12. Edward K. Dienes, R.L.C., Arthur L. Hausberger. Catalyst for the synthesis of methanol. US patent 4,279,781. 1981 Jul 21.
13. Martin, O., et al., *Zinc-Rich Copper Catalysts Promoted by Gold for Methanol Synthesis*. ACS Catalysis, 2015. **5**(9): p. 5607-5616.
14. Khzouz, M., et al., *Characterization and activity test of commercial Ni/Al₂O₃, Cu/ZnO/Al₂O₃ and prepared Ni-Cu/Al₂O₃ catalysts for hydrogen production from methane and methanol fuels*. International Journal of Hydrogen Energy, 2013. **38**: p. 1664–1675.
15. Pokrovski, K.A. and A.T. Bell, *Effect of dopants on the activity of Cu/M_{0.3}Zr_{0.7}O₂ (M = Ce, Mn, and Pr) for CO hydrogenation to methanol*. Journal of Catalysis, 2006. **244**(1): p. 43-51.
16. Bai, Y., et al., *Influences of preparation methods of ZrO₂ support and treatment conditions of Cu/ZrO₂ catalysts on synthesis of methanol via CO hydrogenation*. Catalysis Today, 2010. **149**(1): p. 111-116.
17. Studt, F., et al., *CO hydrogenation to methanol on Cu–Ni catalysts: Theory and experiment*. Journal of Catalysis, 2012. **293**: p. 51-60.
18. Heracleous, E., et al., *Investigation of K-promoted Cu-Zn-Al, Cu-X-Al and Cu-Zn-X (X = Cr, Mn) catalysts for carbon monoxide hydrogenation to higher alcohols*. Applied Catalysis A: General, 2013. **455**: p. 145-154.
19. Anton, J., et al., *Structure–activity relationships of Co-modified Cu/ZnO/Al₂O₃ catalysts applied in the synthesis of higher alcohols from synthesis gas*. Applied Catalysis A: General, 2015. **505**: p. 326-333.
20. Liu, Y.J., et al., *Higher alcohols synthesis via CO hydrogenation on Cu/Zn/Al/Zr catalysts without alkalis and F-T elements*. Fuel Processing Technology, 2016. **144**: p. 186-190.
21. Zhu, Q., Q. Zhang, and L. Wen, *Anti-sintering silica-coating CuZnAlZr catalyst for*

- methanol synthesis from CO hydrogenation*. Fuel Processing Technology, 2016. 156.
22. Qi, G.-X., et al., *Methanol Synthesis by CO₂ Hydrogenation over Titanium Modified γ -Al₂O₃ Supported Copper Catalysts*. Reaction Kinetics and Catalysis Letters, 2001. 73.
 23. Hong, Z.-s., et al., *CO₂ Hydrogenation to Methanol Over Cu/ZnO/Al₂O₃ Catalysts Prepared by a Novel Gel-Network-Coprecipitation Method*. Catalysis Letters, 2002. 82(1): p. 37-44.
 24. Słoczyński, J., et al., *Effect of Mg and Mn oxide additions on structural and adsorptive properties of Cu/ZnO/ZrO₂ catalysts for the methanol synthesis from CO₂*. Applied Catalysis A: General, 2003. 249: p. 129-138.
 25. Ma, Z., et al., *Methanol synthesis from CO₂-rich syngas over a ZrO₂ doped CuZnO catalyst*. Catalysis Today - CATAL TODAY, 2006. 115: p. 222-227.
 26. An, X., et al., *A Cu/Zn/Al/Zr Fibrous Catalyst that is an Improved CO₂ Hydrogenation to Methanol Catalyst*. Catalysis Letters, 2007. 118(3): p. 264-269.
 27. Guo, X., et al., *Combustion synthesis of CuO–ZnO–ZrO₂ catalysts for the hydrogenation of carbon dioxide to methanol*. Catalysis Communications, 2009. 10: p. 1661-1664.
 28. Gao, P., et al., *Influence of modifier (Mn, La, Ce, Zr and Y) on the performance of Cu/Zn/Al catalysts via hydrotalcite-like precursors for CO₂ hydrogenation to methanol*. Applied Catalysis A: General, 2013. 468: p. 442-452.
 29. Liu, Z.-j., et al., *Synthesis and Catalytic Performance of Graphene Modified CuO-ZnO- Al₂O₃ for CO₂ Hydrogenation to Methanol*. Journal of Nanomaterials, 2014. 2014.
 30. Lei, H., Z. Hou, and J. Xie, *Hydrogenation of CO₂ to CH₃OH over CuO/ZnO/Al₂O₃ catalysts prepared via a solvent-free routine*. Fuel, 2016. 164: p. 191-198.
 31. Zhang, C., et al., *Preparation and CO₂ hydrogenation catalytic properties of alumina microsphere supported Cu-based catalyst by deposition-precipitation method*. Journal of CO₂ Utilization, 2017. 17: p. 263-272.

32. Lo, I.C. and H.-S. Wu, *Methanol formation from carbon dioxide hydrogenation using Cu/ZnO/Al₂O₃ catalyst*. Journal of the Taiwan Institute of Chemical Engineers, 2019. **98**: p. 124-131.
33. Ren, S., et al., *Enhanced catalytic performance of Zr modified CuO/ZnO/Al₂O₃ catalyst for methanol and DME synthesis via CO₂ hydrogenation*. Journal of CO₂ Utilization, 2020. **36**: p. 82-95.
34. Kamonlak Pongpanumaporn, E.o.C.Z.A.O.c.m.u.Z., Mn and Si for methanol synthesis via CO₂ hydrogenation (Master's Thesis, Chemical Engineering, Chulalongkorn University, 2020), p.42-43.
35. Allam, D., S. Cheknoun, and S. Hocine, *Operating Conditions and Composition Effect on the Hydrogenation of Carbon Dioxide Performed over CuO/ZnO/Al₂O₃ Catalysts*. Bulletin of Chemical Reaction Engineering & Catalysis, 2019. **14**: p. 604.
36. Arena, F., et al., *Effects of oxide carriers on surface functionality and process performance of the Cu–ZnO system in the synthesis of methanol via CO₂ hydrogenation*. Journal of Catalysis, 2013. **300**: p. 141-151.
37. Lim, H.-W., et al., *Modeling of the Kinetics for Methanol Synthesis using Cu/ZnO/Al₂O₃/ZrO₂ Catalyst: Influence of Carbon Dioxide during Hydrogenation*. Industrial & Engineering Chemistry Research, 2009. **48**(23): p. 10448-10455.
38. Atake, I., et al., *Catalytic behavior of ternary Cu/ZnO/Al₂O₃ systems prepared by homogeneous precipitation in water-gas shift reaction*. Journal of Molecular Catalysis A: Chemical, 2007. **275**(1): p. 130-138.
39. Li, C., X. Yuan, and K. Fujimoto, *Development of highly stable catalyst for methanol synthesis from carbon dioxide*. Applied Catalysis A: General, 2014. **469**: p. 306-311.
40. Meshkini, F., M. Taghizadeh, and M. Bahmani, *Investigating the effect of metal oxide additives on the properties of Cu/ZnO/Al₂O₃ catalysts in methanol synthesis from syngas using factorial experimental design*. Fuel, 2010. **89**(1): p. 170-175.
41. Wang, D., et al., *Characterization and performance of Cu/ZnO/Al₂O₃ catalysts*

- prepared via decomposition of $M(\text{Cu}, \text{Zn})$ -ammonia complexes under sub-atmospheric pressure for methanol synthesis from H_2 and CO_2 . *Journal of Natural Gas Chemistry*, 2011. **20**(6): p. 629-634.
42. Qi, T., et al., *Yttria-doped Cu/ZnO catalyst with excellent performance for CO_2 hydrogenation to methanol*. *Molecular Catalysis*, 2021. **509**: p. 111641.
 43. Zhu, L., et al., *Synthesis of 0D/3D CuO/ZnO Heterojunction with Enhanced Photocatalytic Activity*. *The Journal of Physical Chemistry C*, 2018. **122**.
 44. Dow, W.-P., Y.-P. Wang, and T.-J. Huang, *TPR and XRD studies of yttria-doped ceria/[gamma]-alumina-supported copper oxide catalyst*. *Applied Catalysis A: General*, 2000. **190**: p. 25-34.
 45. Wang, W., et al., *An investigation of Zr/Ce ratio influencing the catalytic performance of $\text{CuO}/\text{Ce}_{1-x}\text{Zr}_x\text{O}_2$ catalyst for CO_2 hydrogenation to CH_3OH* . *Journal of Energy Chemistry*, 2020. **47**: p. 18-28.
 46. Kang, R., et al., *Reaction mechanism and kinetics of CO oxidation over a $\text{CuO}/\text{Ce}_{0.75}\text{Zr}_{0.25}\text{O}_2$ - δ catalyst*. *Applied Catalysis A: General*, 2018. **565**: p. 46-58.
 47. Zhang, Y., et al., *Catalytic performance of spray-dried $\text{Cu}/\text{ZnO}/\text{Al}_2\text{O}_3/\text{ZrO}_2$ catalysts for slurry methanol synthesis from CO_2 hydrogenation*. *Journal of CO_2 Utilization*, 2016. **15**: p. 72-82.
 48. Shi, Z., Q. Tan, and D. Wu, *Ternary copper-cerium-zirconium mixed metal oxide catalyst for direct CO_2 hydrogenation to methanol*. *Materials Chemistry and Physics*, 2018. **219**: p. 263-272.
 49. Tripathi, K., et al., *Origin of MnO induced Cu_0/Cu + surface active centers for CO_2 containing syngas conversion to DME via tandem catalysis*. *Sustainable Energy & Fuels*, 2021. **5**.
 50. Sharafutdinov, I., *Investigations into low pressure methanol synthesis*. 2013. p. 98.
 51. Al-Fatesh, A.S., et al., *Combined magnesia, ceria and nickel catalyst supported over γ -alumina doped with titania for dry reforming of methane*. *Catalysts*, 2019. **9**(2).

52. Chen, F., et al., *Ni-Cu bimetallic catalysts on Yttria-stabilized zirconia for hydrogen production from ethanol steam reforming*. *Fuel*, 2020. 280.





จุฬาลงกรณ์มหาวิทยาลัย
CHULALONGKORN UNIVERSITY

VITA

NAME	Phapatchaya Phonrat
DATE OF BIRTH	13 June 1995
PLACE OF BIRTH	Bangkok
INSTITUTIONS ATTENDED	Department of Chemical Engineering, Faculty of Engineering, Chulalongkorn University

